A proposal for realizing Majorana fermions in strongly correlated wires

Kaushal Kumar Kesharpu

BLTP, JINR, DUBNA

- K. K. Kesharpu, E. A. Kochetov, and A. Ferraz, **Physical Review B 107, 155146 (2023)**
- K. K. Kesharpu, **arxiv:2305.13423 (2023)** (PRB second round review**)**
- K. K. Kesharpu, E. A. Kochetov, and A. Ferraz, A proposal for realizing Majorana fermions without magnetic field in strongly correlated nanowires **(2023)** (PRB first round review)

JINR- October 2023

Plan of the presentation

Introduction

Majorana Fermions

a. What are **Majorana fermions**?

b. How to **realize** them in **condensed matter physics**?

c. What are the **devices synthesized** until now**,** and their **drawbacks**?

The first mention of Majorana Particles

Majorana, E. (1937) Il Nuovo Cimento, 5, 171-184.

1937

Ettore Majorana

The first mention of Majorana Particles

1937

Ettore Majorona

The antiparticle of a **Dirac** particle is **different.**

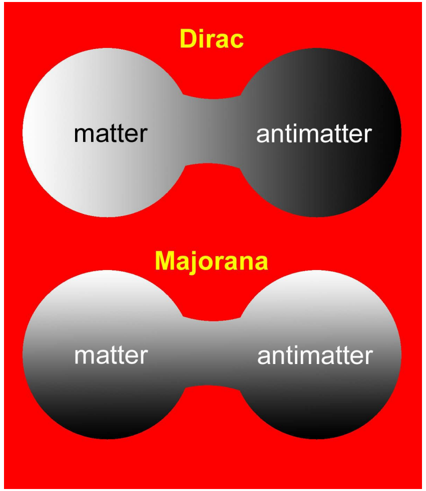

The antiparticle of a **Majorana** particle is **same.**

Properties of the Majorana operators

1937

Ettore Majorana

Mathematically:
If ***a*** is some operator of **Majorana particle** then:

$$a_i = a_i^\dagger$$

Majorana operators in terms of the fermion operators

$$a_i = f_i + f_i^\dagger$$

$$a_j^\dagger = \imath \left(f_j - f_j^\dagger \right)$$

Until now **no fundamental particle** has this property !

1937

Ettore Majorana

Majorana intended this idea for application in particle physics, especially, he proposed **neutrinos to be its own antiparticle.** However, until now experimentally it is **not found**. Supersymmetric theories proposes that, bosonic particles like **photons** might be **Majorana particles**.

However !!!

Fundamental excitation in condensed matter physics gives a way out !

1937

Ettore Majorana

However !!!

In condensed matter physics **interaction induced excitations** can be thought as **particle**, hence, ingenious combination of **symmetries and excitations** can give rise to Majorana particles. **Defects** can also supports Majorana particles.

Majorana zero-modes (MZM) in 1D systems

2001

Alexei Kitaev

Kitaev A Y, Phys.–Usp. (44) 131, 2001

A chain of atoms with **p-wave** superconducting gap

2010

Yuval Oreg

Yuval Oreg et. al.,Phys. Rev. Lett. 105, 177002

Showed a nanowire with **spin-orbit** and **zeeman** coupling develops MZM

2010

Jay D. Sau

Sankar Das Sarma

Roman M. Lutchyn et al., Phys. Rev. Lett. 105, 077001

Proposed working device concept with **semiconductor (InAs)** which has strong **spin-orbit** coupling

Kitaev toy model

2001

Alexei Kitaev

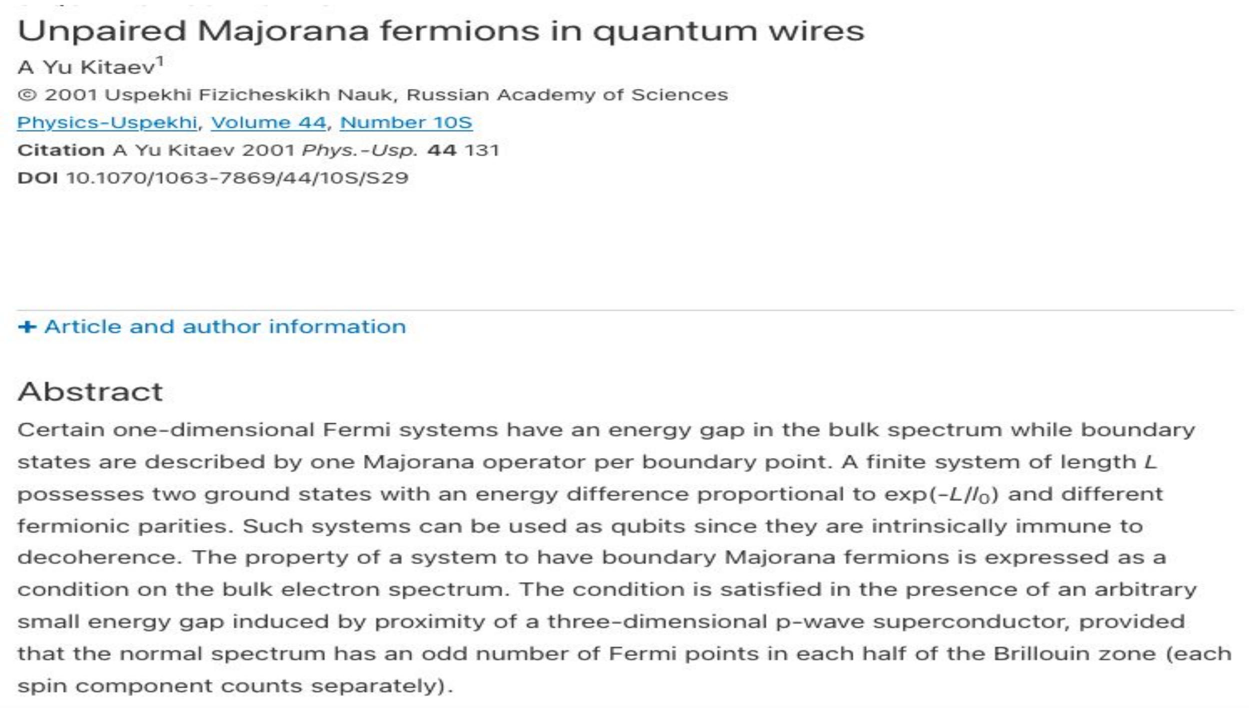

Unpaired Majorana fermions in quantum wires

A Yu Kitaev[1]

© 2001 Uspekhi Fizicheskikh Nauk, Russian Academy of Sciences

Physics-Uspekhi, Volume 44, Number 10S

Citation A Yu Kitaev 2001 *Phys.-Usp.* **44** 131

DOI 10.1070/1063-7869/44/10S/S29

+ Article and author information

Abstract

Certain one-dimensional Fermi systems have an energy gap in the bulk spectrum while boundary states are described by one Majorana operator per boundary point. A finite system of length L possesses two ground states with an energy difference proportional to $\exp(-L/l_0)$ and different fermionic parities. Such systems can be used as qubits since they are intrinsically immune to decoherence. The property of a system to have boundary Majorana fermions is expressed as a condition on the bulk electron spectrum. The condition is satisfied in the presence of an arbitrary small energy gap induced by proximity of a three-dimensional p-wave superconductor, provided that the normal spectrum has an odd number of Fermi points in each half of the Brillouin zone (each spin component counts separately).

It was shown that, Majorana zero modes may appear in the 1D wire with p-wave superconducting order parameter.

Kitaev toy model

2001

Alexei Kitaev

We begin by reviewing Kitaev's toy lattice model [9], introduced nearly a decade ago, for a 1D spinless p-wave superconductor. This model's many virtues include the fact that in this setting Majorana zero-modes appear in an extremely simple and intuitive fashion. Following Kitaev, we introduce operators c_x describing spinless fermions that hop on an N-site chain and exhibit long-range-ordered p-wave superconductivity. The minimal Hamiltonian describing this setup reads

$$H = -\mu \sum_x c_x^\dagger c_x - \frac{1}{2} \sum_x (t c_x^\dagger c_{x+1} + \Delta e^{i\phi} c_x c_{x+1} + \text{H.c.}), \quad (2)$$

where μ is the chemical potential, $t \geqslant 0$ is the nearest-neighbor hopping strength, $\Delta \geqslant 0$ is the p-wave pairing amplitude and

Kitaev toy model

2001

Alexei Kitaev

$$c_x = \frac{e^{-i\phi/2}}{2}(\gamma_{B,x} + i\gamma_{A,x}). \quad (14)$$

The operators on the right-hand side obey the canonical Majorana fermion relations

$$\gamma_{\alpha,x} = \gamma_{\alpha,x}^{\dagger}, \qquad \{\gamma_{\alpha,x}, \gamma_{\alpha',x'}\} = 2\delta_{\alpha\alpha'}\delta_{xx'}. \quad (15)$$

In this basis H becomes

$$H = -\frac{\mu}{2}\sum_{x=1}^{N}(1 + i\gamma_{B,x}\gamma_{A,x}) - \frac{i}{4}\sum_{x=1}^{N-1}[(\Delta + t)\gamma_{B,x}\gamma_{A,x+1} + (\Delta - t)\gamma_{A,x}\gamma_{B,x+1}]. \quad (16)$$

Kitaev toy model

$$H = -\frac{\mu}{2}\sum_{x=1}^{N}(1 + \mathrm{i}\gamma_{B,x}\gamma_{A,x}) - \frac{\mathrm{i}}{4}\sum_{x=1}^{N-1}[(\Delta + t)\gamma_{B,x}\gamma_{A,x+1} + (\Delta - t)\gamma_{A,x}\gamma_{B,x+1}]. \quad (16)$$

Kitaev toy model

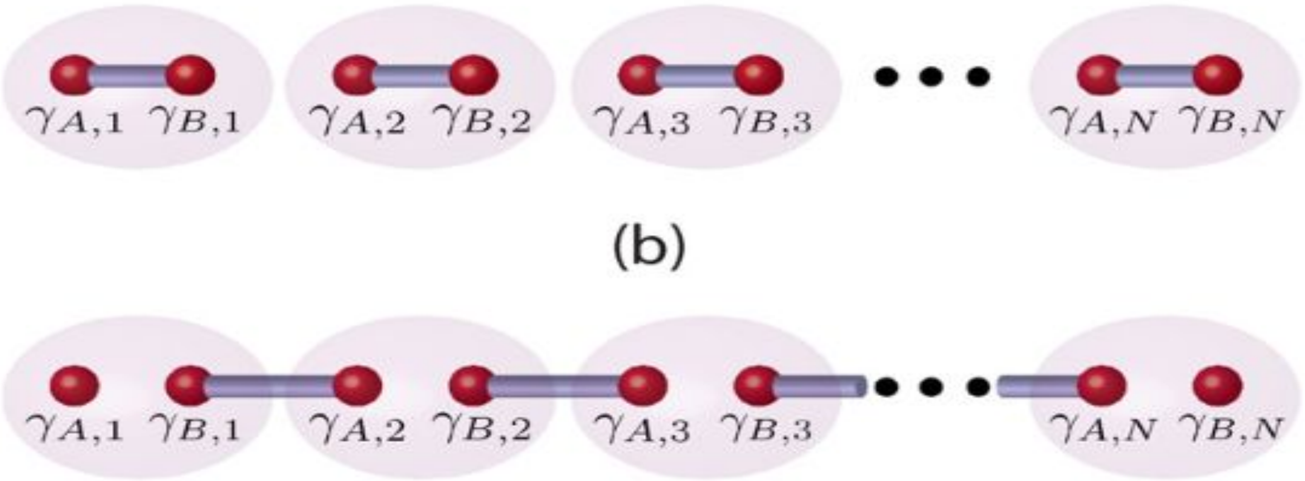

Figure 2. Schematic illustration of the Hamiltonian in equation (16) when (*a*) $\mu \neq 0, t = \Delta = 0$ and (*b*) $\mu = 0, t = \Delta \neq 0$. In the former limit Majoranas 'pair up' at the same lattice site, resulting in a unique ground state with a gap to all excited states. In the latter, Majoranas couple at adjacent lattice sites, leaving two 'unpaired' Majorana zero-modes $\gamma_{A,1}$ and $\gamma_{B,N}$ at the ends of the chain. Although there remains a bulk energy gap in this case, these end states give rise to a two-fold ground-state degeneracy.

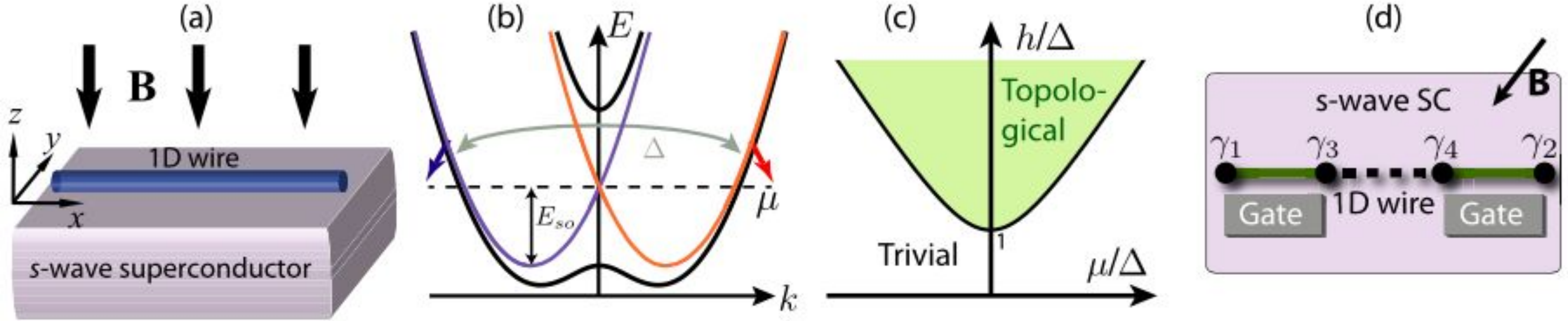

Figure 6. (*a*) Basic architecture required to stabilize a topological superconducting state in a 1D spin–orbit-coupled wire. (*b*) Band structure for the wire when time-reversal symmetry is present (red and blue curves) and broken by a magnetic field (black curves). When the chemical potential lies within the field-induced gap at $k = 0$, the wire appears 'spinless'. Incorporating the pairing induced by the proximate superconductor leads to the phase diagram in (*c*). The endpoints of topological (green) segments of the wire host localized, zero-energy Majorana modes as shown in (*d*).

Three ingredients are necessary:

1. **Strong Rashba spin-orbit coupling**
2. **Broken time reversal symmetry**
3. **s-wave superconductors**

Jay D. Sau

Sankar Das Sarma

Roman M. Lutchyn et al., **Phys. Rev. Lett. 105, 077001**

Yuval Oreg et. al.,Phys. **Rev. Lett. 105, 177002**

Microsoft Azure device

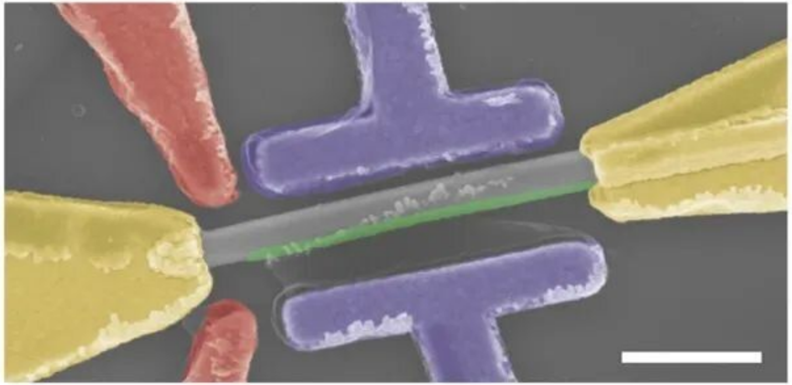

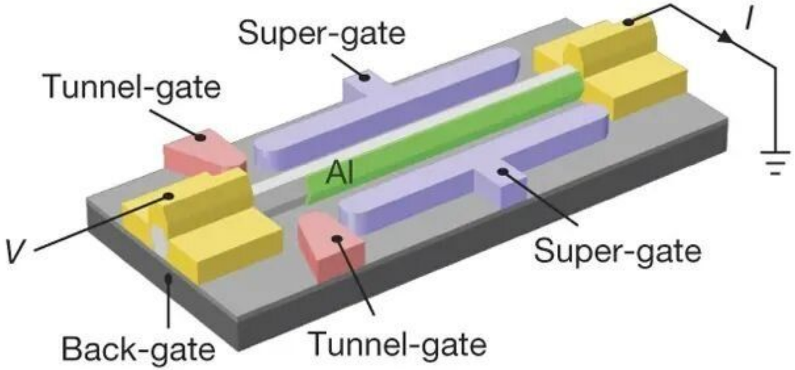

The building blocks of quantum computer

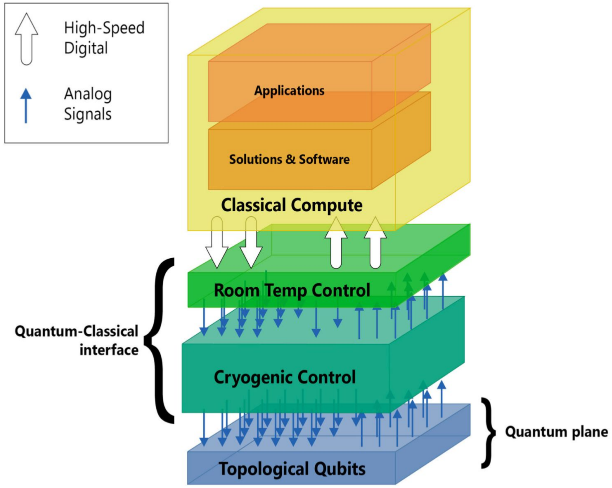

The main problems in superconductor-semiconductor Heterostructures

- Use of **magnetic field,** which might **destroy** the s-wave superconductivity
- **Strong Rashba spin-orbit** coupling, so that for small magnetic field a large superocnducting gap is opened
- **Low superconducting transition temperature** of s-wave superconductors

Table 1 | **Bulk properties of semiconductors**[46,186,187]

Bulk properties	InAs	InSb
g-Factor	8–15	40–50
Effective mass m^*, m_e	0.023	0.014
Spin–orbit energy, meV	0.05–1	0.05–1
Spin–orbit coupling α, eV Å	0.2–0.8	0.2–1
Spin–orbit length, nm	180–40	230–50

Rashba spin–orbit coupling strength was measured in nanoscale structures[84,107]. m_e is the electron mass; $E_{SO}=\frac{m^*\alpha^2}{2\hbar^2}$ is the spin–orbit energy; $\lambda_{SO}\equiv k_{SO}^{-1}=\frac{\hbar^2}{\alpha m^*}$ is the spin–orbit length.

Table 2 | **Bulk properties of superconductors**[46,187,188]

Bulk properties	Al	NbTiN
Superconducting gap Δ	0.2 meV	3 meV
Critical field B_c	10 mT	10 T
Critical temperature T_c	1.2 K	15 K

Our Proposal

The System

We consider a 1D nanowire with **strong correlation** on the ***extended s***-wave superconductor.

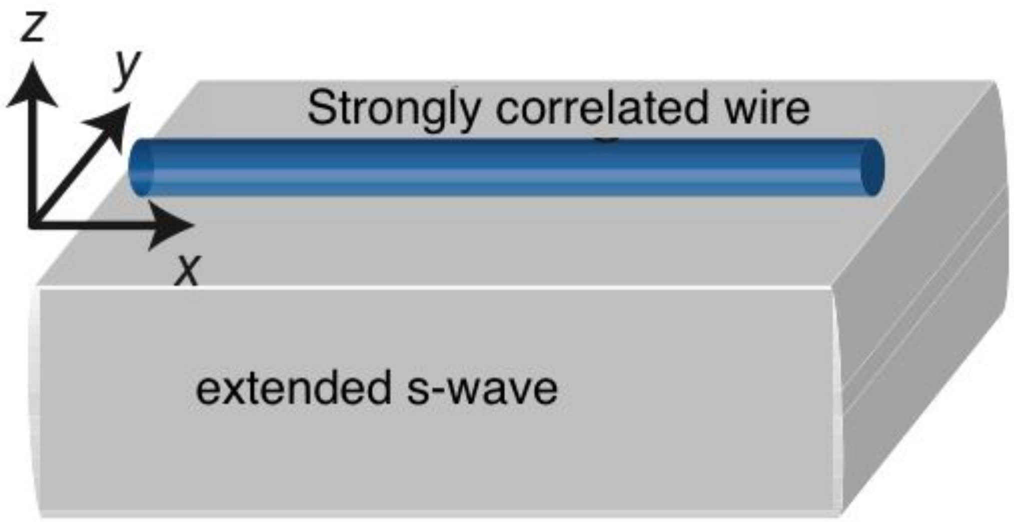

Coulomb interaction is much **higher** than the **kinetic energy** of the electrons

$$U \gg t$$

Extended s-wave superconductors have **Momentum dependent** superconducting gap

$$\Delta = \Delta_0 \sin k_x$$

How our system is different from previously proposed systems?

Our Proposal

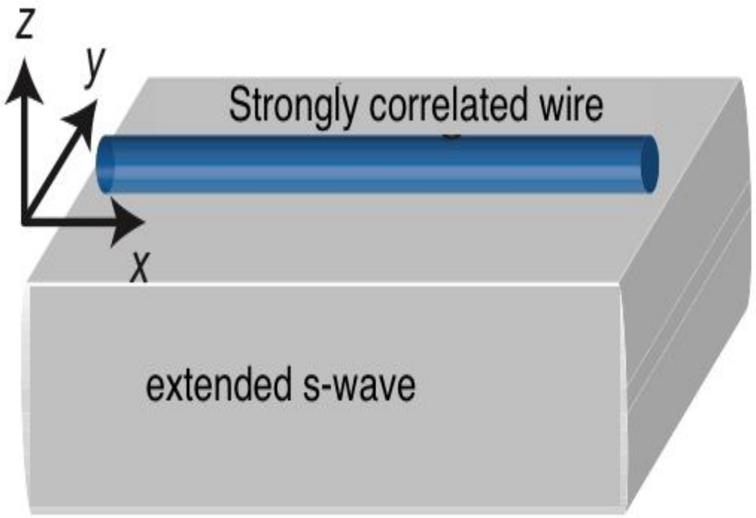

Jay D. Sau et. al., Phys. Rev. Lett. 104, 040502

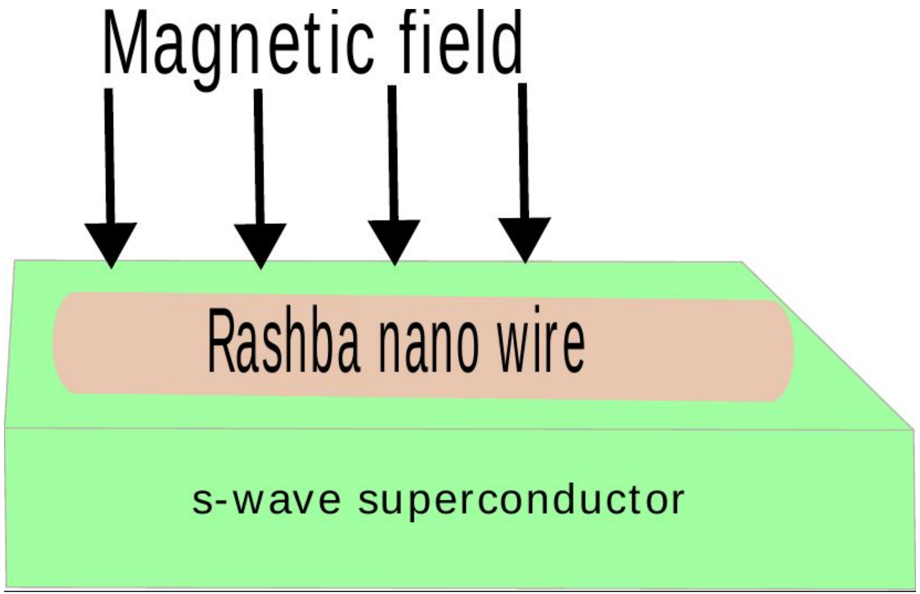

The Hamiltonian of the whole system

The total Hamiltonian of the system contains:

1. Hamiltonian of the **1D nanowire**

2. Hamiltonian of the **substrate superconductor**

Proximity induced superconducting in wire

Due to **proximity effect** superconductivity will also be induced in the nano wire.

Both **Andreev reflection** and **coherent propagation** of the superconducting pairs are responsible for induced superconductivity.

We assume **superconducting coherence length** is of **same order** as the **radius of the wire** ($\xi_{\text{wire}} \sim r$).

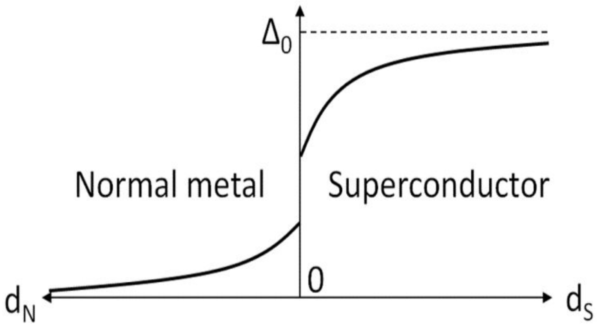

Coherent propagation

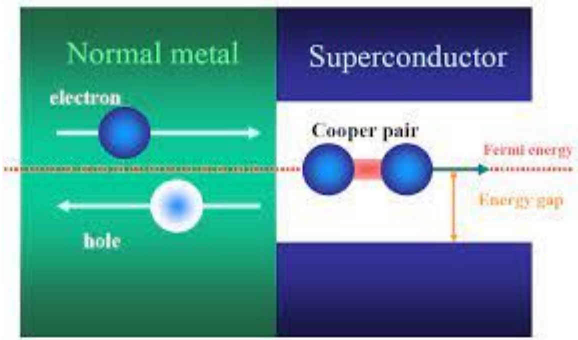

Andreev Reflection

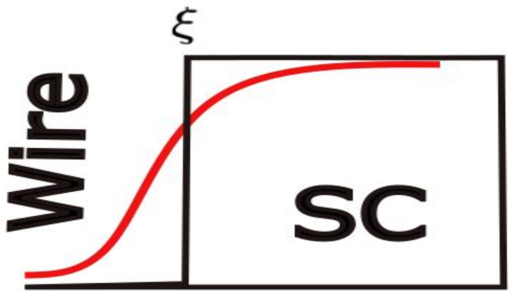

The Hamiltonian of the wire

The Hamitonian of the wire contains four terms:

1. The **kinetic energy** term
2. The **superconducting** term with **extended s-wave** order parameters
3. The **Rashba spin orbit** term (just for generality, although, not necessary)
4. The **chemical potential** term

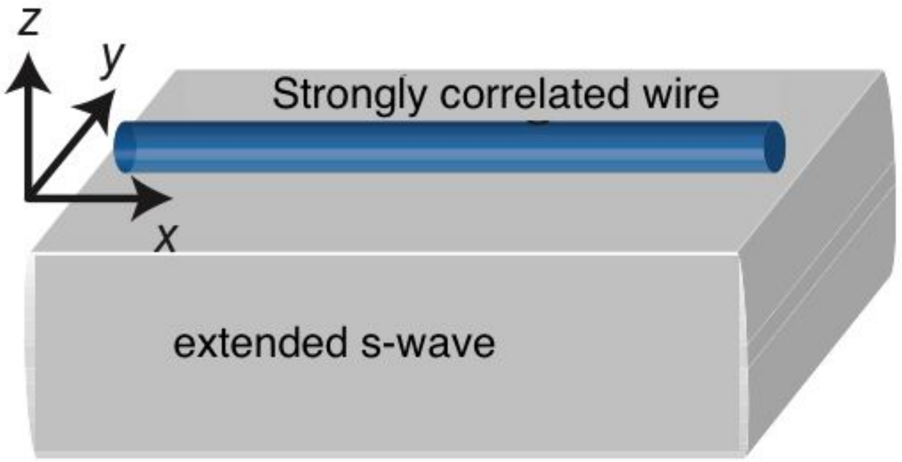

Due to strong correlation X operators will be used

1D nano wire with **strong electron-electron** coulomb repulsion ($U \approx \infty$).

In this case the **Hamiltonian will be represented** by the X_i^{pq} operators. It is the transition of the electrons from state $|q\rangle$ to $\langle p|$

If $c_{i,\sigma}$ is the **usual electron** operator, and $\hat{n}_{i,\sigma} = \hat{c}_{i,\sigma}^{\dagger}\hat{c}_{i,\sigma}$ is the **electron number** operator, then:

$$X_i^{0\sigma} = c_{i\sigma}(1 - n_{i\sigma'}), \quad X_i^{\sigma 0} = (1 - n_{i\sigma'})c_{i\sigma}^{\dagger}$$

$$X_i^{00} = 1 - \sum_{\sigma} (1 - n_{i\sigma'})\, c_{i\sigma}^{\dagger} c_{i\sigma}^{\dagger}\, (1 - n_{i\sigma'})\,.$$

The Kinetic energy term

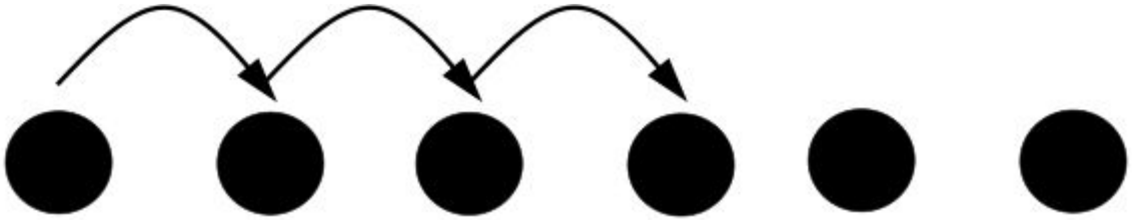

$$H_{1D} = -t \sum_i X_i^{\sigma 0} X_{i+1}^{0\sigma} + X_i^{\sigma' 0} X_{i+1}^{0\sigma'} + \text{H.c}$$

where,

$X_i^{\sigma,\sigma'}$ = Transition of state at i-th site from σ to σ' spin state

The Rashba Spin-orbit coupling

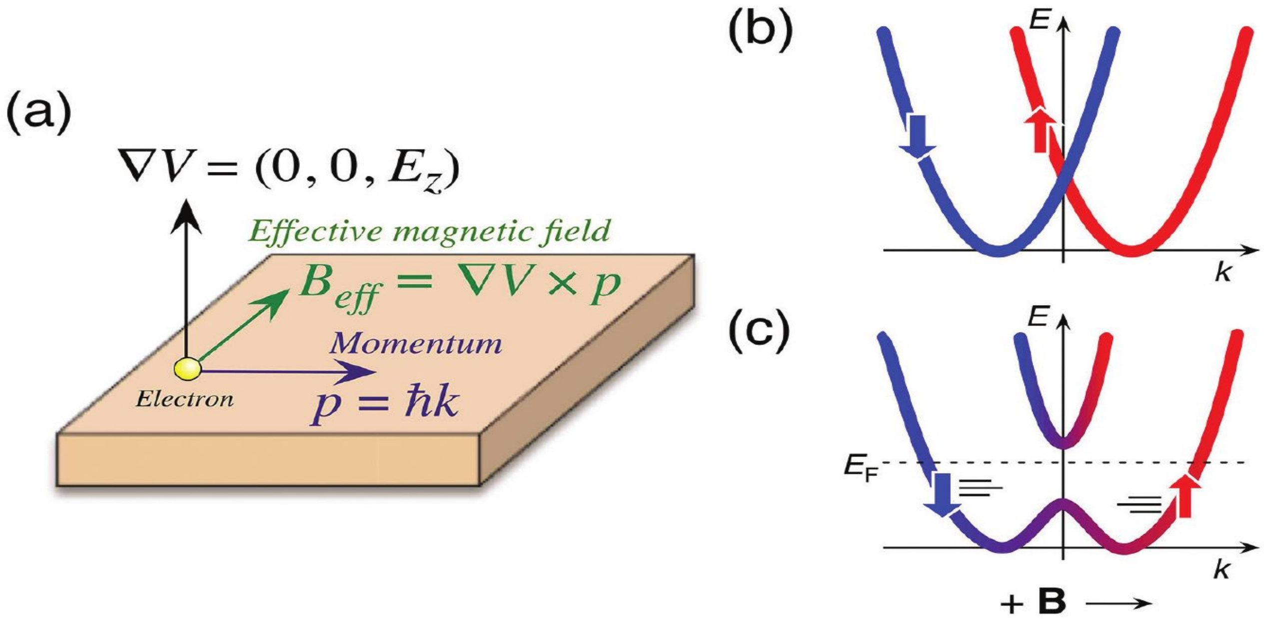

$$H_\alpha = -\imath\alpha \sum_i X_i^{\sigma'0} X_{i+1}^{0\sigma} - X_i^{\sigma 0} X_{i+1}^{0\sigma'} + \mathrm{H.c}$$

The Superconducting term

$$H_\Gamma \approx \Delta \sum_i X_i^{\sigma 0} X_{i+1}^{\sigma' 0} - X_i^{\sigma' 0} X_{i+1}^{\sigma 0} + \text{H.c.}$$

The Total Hamiltonian

$$
\begin{aligned}
H_{\text{eff}} = & - t \sum_i X_i^{\sigma 0} X_{i+1}^{0\sigma} + X_i^{\sigma' 0} X_{i+1}^{0\sigma'} \\
& - \imath\alpha \sum_i X_i^{\sigma' 0} X_{i+1}^{0\sigma} - X_i^{\sigma 0} X_{i+1}^{0\sigma'} \\
& + \Delta \sum_i X_i^{\sigma 0} X_{i+1}^{\sigma' 0} - X_i^{\sigma' 0} X_{i+1}^{\sigma 0} + \text{H.c.} \\
& + \mu \sum_i X_i^{00}.
\end{aligned}
$$

Fractionalization of the electrons

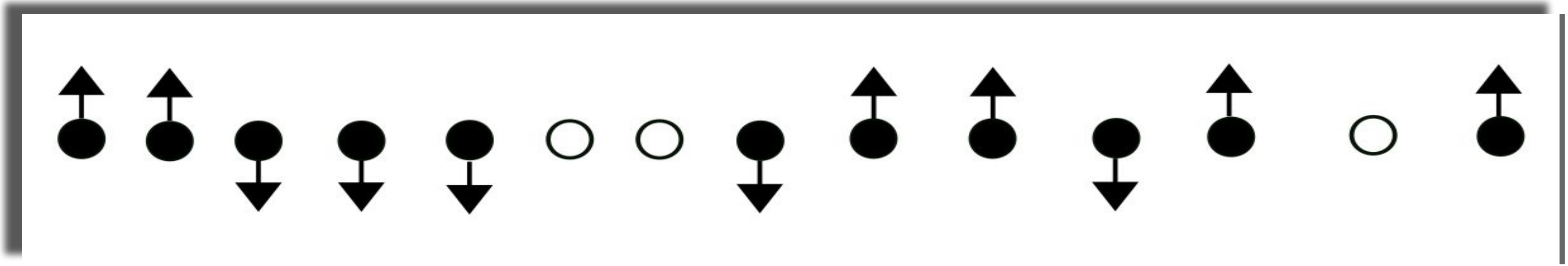

How to solve the Hamiltonian???

Through Fractionalization of the electrons

Fractionalization of the electrons

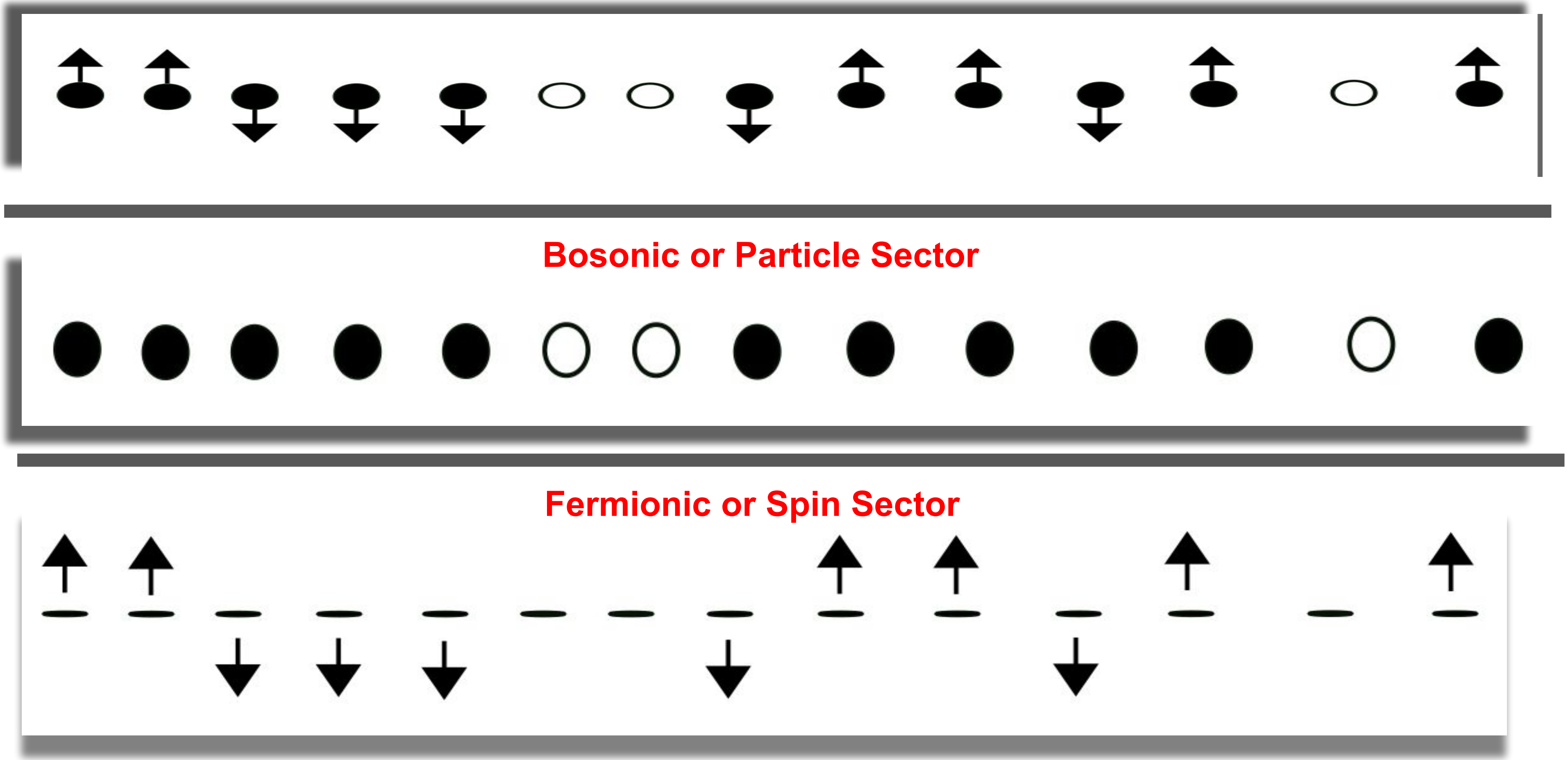

su(2|1) coherent state symbols of X operators

The CS symbols of the X operators, $X_{cs} = \langle z, \xi | X | z, \xi \rangle$, read

$$X_{cs}^{0\downarrow} = -\frac{z\bar{\xi}}{1+|z|^2}, \quad X_{cs}^{\downarrow 0} = -\frac{\bar{z}\xi}{1+|z|^2},$$

$$X_{cs}^{0\uparrow} = -\frac{\bar{\xi}}{1+|z|^2}, \quad X_{cs}^{\uparrow 0} = -\frac{\xi}{1+|z|^2},$$

$$Q_{cs}^{+} = X_{cs}^{\uparrow\downarrow} = \frac{z}{1+|z|^2}\left(1 - \frac{\bar{\xi}\xi}{1+|z|^2}\right),$$

$$Q_{cs}^{-} = X_{cs}^{\downarrow\uparrow} = \frac{\bar{z}}{1+|z|^2}\left(1 - \frac{\bar{\xi}\xi}{1+|z|^2}\right),$$

$$Q_{cs}^{z} = \frac{1}{2}(X_{cs}^{\uparrow\uparrow} - X_{cs}^{\downarrow\downarrow}) = \frac{1}{2}\frac{1-|z|^2}{1+|z|^2}\left(1 - \frac{\bar{\xi}\xi}{1+|z|^2}\right). \quad (3)$$

There is a one-to-one correspondence between the $su(2|1)$ generators and their CS symbols [5].

z :A complex number

The bosonic field

ξ :A Grassman paramter

The fermionic field

Hamiltonian in terms of the Coherent state symbols

$$H_{\mathrm{eff}}(z,\xi) = -\,t\sum_i \xi_i \bar{\xi}_{i+1} a_{i,i+1} + \imath\alpha \sum_i \xi_i \bar{\xi}_{i+1} \alpha^*_{i,i+1} - \Delta \sum_i \xi_i \xi_{i+1} \Delta^*_{i,i+1} + \mathrm{H.c.} + \mu \sum_i \bar{\xi}_i \xi_i ,$$

Hamiltonian in terms of the Coherent state symbols

$$H_{\text{eff}}(z,\xi) = -\,t\sum_i \xi_i\bar{\xi}_{i+1} a_{i,i+1} + \imath\alpha\sum_i \xi_i\bar{\xi}_{i+1}\alpha^*_{i,i+1} - \Delta\sum_i \xi_i\xi_{i+1}\Delta^*_{i,i+1} + \text{H.c.} + \mu\sum_i \bar{\xi}_i\xi_i,$$

$$a_{i,i+1} \equiv \frac{1+\bar{z}_i z_{i+1}}{\sqrt{\left(1+|z_i|^2\right)\left(1+|z_{i+1}|^2\right)}},$$

Hamiltonian in terms of the Coherent state symbols

$$H_{\text{eff}}(z,\xi) = -t\sum_i \xi_i\bar{\xi}_{i+1}a_{i,i+1} + \imath\alpha\sum_i \xi_i\bar{\xi}_{i+1}\alpha^*_{i,i+1}$$
$$-\Delta\sum_i \xi_i\xi_{i+1}\Delta^*_{i,i+1} + \text{H.c.} + \mu\sum_i \bar{\xi}_i\xi_i,$$

$$\alpha^*_{i,i+1} \equiv \left[\frac{z_i - \bar{z}_{i+1}}{\sqrt{\left(1+|z_i|^2\right)\left(1+|z_{i+1}|^2\right)}}\right]^*$$

Hamiltonian in terms of the Coherent state symbols

$$H_{\text{eff}}(z,\xi) = -\,t\sum_i \xi_i \bar{\xi}_{i+1} a_{i,i+1} + \imath\alpha \sum_i \xi_i \bar{\xi}_{i+1} \alpha^*_{i,i+1}$$

$$-\,\Delta \sum_i \xi_i \xi_{i+1} \boxed{\Delta^*_{i,i+1}} + \text{H.c.} + \mu \sum_i \bar{\xi}_i \xi_i ,$$

$$\Delta^*_{i,i+1} \equiv \left[\frac{z_i - z_{i+1}}{\sqrt{\left(1+|z_i|^2\right)\left(1+|z_{i+1}|^2\right)}} \right]^* .$$

Hamiltonian in terms of the Coherent state symbols

$$\begin{aligned}H_{\text{eff}}(z,\xi) = &- t\sum_i \xi_i\bar{\xi}_{i+1}a_{i,i+1} + \imath\alpha\sum_i \xi_i\bar{\xi}_{i+1}\alpha^*_{i,i+1} \\ &- \Delta\sum_i \xi_i\xi_{i+1}\Delta^*_{i,i+1} + \text{H.c.} + \mu\sum_i \bar{\xi}_i\xi_i,\end{aligned} \tag{7}$$

where,

$$a_{i,i+1} \equiv \frac{1+\bar{z}_i z_{i+1}}{\sqrt{\left(1+|z_i|^2\right)\left(1+|z_{i+1}|^2\right)}}, \tag{8a}$$

$$\alpha^*_{i,i+1} \equiv \left[\frac{z_i-\bar{z}_{i+1}}{\sqrt{\left(1+|z_i|^2\right)\left(1+|z_{i+1}|^2\right)}}\right]^*, \tag{8b}$$

$$\Delta^*_{i,i+1} \equiv \left[\frac{z_i-z_{i+1}}{\sqrt{\left(1+|z_i|^2\right)\left(1+|z_{i+1}|^2\right)}}\right]^*. \tag{8c}$$

Results

Spin spiral (helical) texture

$$\vec{S}_i = (S_i^x, S_i^y, S_i^z) = \frac{1}{2}(\cos\theta_i, \sin\theta_i, 0)\,.$$

Schematic of system with spiral spin structures

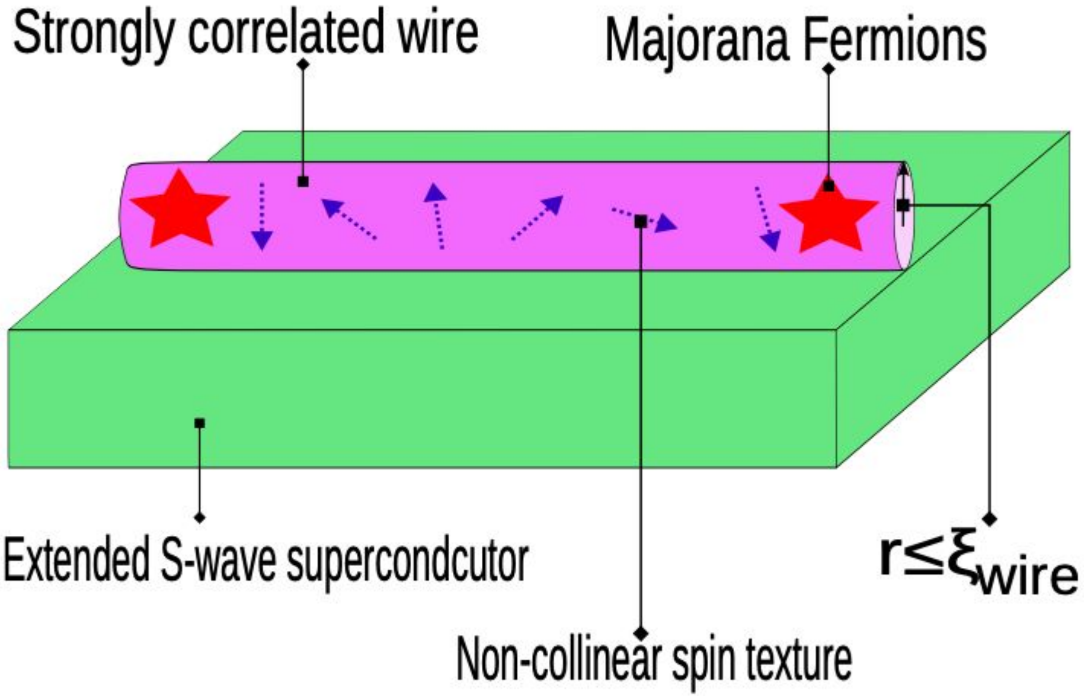

Spin spiral (helical) texture in experiments

PRL **105,** 177002 (2010) PHYSICAL REVIEW LETTERS week ending 22 OCTOBER 2010

Helical Liquids and Majorana Bound States in Quantum Wires

Yuval Oreg,[1] Gil Refael,[2] and Felix von Oppen[3]

[1]*Department of Condensed Matter Physics, Weizmann Institute of Science, Rehovot, 76100, Israel*
[2]*Department of Physics, California Institute of Technology, Pasadena, California 91125, USA*
[3]*Dahlem Center for Complex Quantum Systems and Fachbereich Physik, Freie Universität Berlin, 14195 Berlin, Germany*

(Received 16 March 2010; published 20 October 2010)

We show that the combination of spin-orbit coupling with a Zeeman field or strong interactions may lead to the formation of a helical electron liquid in single-channel quantum wires, with spin and velocity perfectly correlated. We argue that zero-energy Majorana bound states are formed in various situations when such wires are situated in proximity to a conventional s-wave superconductor. This occurs when the external magnetic field, the superconducting gap, or, most simply, the chemical potential vary along the wire. These Majorana states do not require the presence of a vortex in the system. Experimental consequences of the helical liquid and the Majorana states are also discussed.

DOI: 10.1103/PhysRevLett.105.177002 PACS numbers: 74.78.Na, 03.67.Lx, 73.63.Nm, 74.78.Fk

PHYSICAL REVIEW B **90**, 165136 (2014)

Rashba spin-orbit coupling in the Kane-Mele-Hubbard model

Manuel Laubach,[1] Johannes Reuther,[2] Ronny Thomale,[1] and Stephan Rachel[3]

[1]*Institute for Theoretical Physics, University of Würzburg, 97074 Würzburg, Germany*
[2]*Department of Physics, California Institute of Technology, Pasadena, California 91125, USA*
[3]*Institute for Theoretical Physics, Technische Universität Dresden, 01062 Dresden, Germany*

(Received 18 December 2013; revised manuscript received 10 October 2014; published 27 October 2014)

V. CONCLUSIONS

We investigated the effect of Rashba spin-orbit coupling in the Kane-Mele-Hubbard model as a prototypical correlated topological insulator. We applied the variational cluster approach and determined the phase diagram via the computation of local density of states, magnetization, single-particle spectral function, and edge states to detect the topological character. The topological-insulating phase persists in the presence of Rashba spin-orbit coupling and interactions. Furthermore, in the strong-coupling regime, the Rashba term induces magnetic frustration which leads to incommensurability effects in the magnetic fluctuation profile and is conjectured to predominantly give rise to spiral magnetic phases. Rashba spin-orbit coupling also gives rise to peculiar metallic phases. We find a weak topological-semiconductor phase, for a wide range of Hubbard interaction strengths as well as intrinsic and Rashba spin-orbit couplings. It will be exciting to investigate some of these effects in future experiments which exhibit the Rashba term due to external fields or intrinsic environmental effects.

Spin spiral (helical) texture in experiments

PHYSICAL REVIEW B **106**, 104503 (2022)

Prevalence of trivial zero-energy subgap states in nonuniform helical spin chains on the surface of superconductors

Richard Hess, Henry F. Legg, Daniel Loss, and Jelena Klinovaja
Department of Physics, University of Basel, Klingelbergstrasse 82, CH-4056 Basel, Switzerland

(Received 6 April 2022; revised 27 June 2022; accepted 9 August 2022; published 8 September 2022)

Helical spin chains, consisting of magnetic (ad)atoms, on the surface of bulk superconductors are predicted to host Majorana bound states (MBSs) at the ends of the chain. Here, we investigate the prevalence of trivial zero-energy bound states in these helical spin-chain systems. The existence of trivial zero-energy bound states can prevent the conclusive identification of MBSs and, given the limited tunability of atomic spin-chain systems, could present a major experimental roadblock. First, we show that the Hamiltonian of a helical spin chain with varying nonuniform rotation rate between neighboring magnetic moments on a superconductor can be mapped to an effective Hamiltonian reminiscent of a ferromagnetic chain with strong Rashba spin-orbit coupling and with smooth nonuniform chemical potential, reminding a Rashba nanowire setups. Previously it has been found that trivial zero-energy states are abundant in nanowire systems with smoothly changing potentials. Therefore, we perform an extensive search for zero-energy bound states in helical spin-chain systems with varying rotation rates. Although bound states with near zero energy do exist for certain dimensionalities and rotation profiles, we find that zero-energy bound states are far less prevalent than in semiconductor nanowire systems with equivalent nonuniformities. In particular, utilizing varying rotation rates, we do not find zero-energy bound states in the most experimentally relevant setup consisting of a one-dimensional helical spin chain on the surface of a three-dimensional superconductor, even for profiles that produce near zero-energy states in equivalent one- and two-dimensional systems. Although our findings do not rule them out, the much reduced prevalence of zero-energy bound states in long nonuniform helical spin chains compared with equivalent semiconductor nanowires, as well as the ability to measure states locally via scanning tunneling microscopy, should reduce the experimental barrier to identifying MBSs in such systems.

DOI: 10.1103/PhysRevB.106.104503

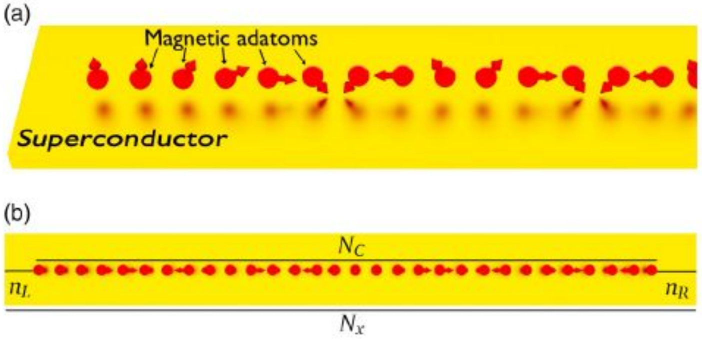

FIG. 1. *Helical spin-chain system.* (a) Magnetic adatoms (red) are placed on the surface of a bulk superconductor (yellow). The adatoms form a helical spin chain with a rotation rate that can vary along the chain. (b) Geometry of helical spin chain used in this paper (number of sites shown is not to scale). The full system has N_x sites in the x direction with magnetic adatoms deposited on N_C sites forming a helical spin chain. In general, the helical spin chain is embedded in the underlying superconductor with n_L sites on the left side of the system and n_R on the right. In addition, we will consider one-, two-, and three-dimensional superconductors underlying the chain.

Spin spiral (helical) texture in experiments

nature reviews materials

Explore content ⌄ About the journal ⌄ Publish with us ⌄

nature > nature reviews materials > review articles > article

Review Article | Published: 06 July 2021

Engineered platforms for topological superconductivity and Majorana zero modes

Karsten Flensberg, Felix von Oppen & Ady Stern

Nature Reviews Materials **6**, 944–958 (2021) | Cite this article

Abstract

Among the major avenues that are being pursued for realizing quantum bits, the Majorana-based approach has been the most recent to be launched. It attempts to realize qubits that store quantum information in a topologically protected manner. The quantum information is protected by non-local storage in localized and well-separated Majorana zero modes, and manipulated by exploiting their non-abelian quantum statistics. Realizing these topological qubits is experimentally challenging, requiring superconductivity, helical electrons (created by spin–orbit coupling) and breaking of time-reversal symmetry to all cooperate in an uncomfortable alliance. Over the past decade, several candidate materials systems for realizing Majorana-based topological qubits have been explored, and there is accumulating, though still debated, evidence that zero modes are indeed being realized. This Review surveys the basic physical principles on which these approaches are based, the materials systems that are being developed and the current state of the field. We highlight both the progress that has been made and the challenges that still need to be overcome.

PHYSICAL REVIEW B **82**, 045127 (2010)

Spin-selective Peierls transition in interacting one-dimensional conductors with spin-orbit interaction

Bernd Braunecker,[1] George I. Japaridze,[2,3] Jelena Klinovaja,[1] and Daniel Loss[1]
[1]*Department of Physics, University of Basel, Klingelbergstrasse 82, 4056 Basel, Switzerland*
[2]*Andronikashvili Institute of Physics, Tamarashvili 6, 0177 Tbilisi, Georgia*
[3]*Ilia State University, Cholokashvili Ave. 3-5, 0162 Tbilisi, Georgia*
(Received 7 July 2010; published 29 July 2010)

Interacting one-dimensional conductors with Rashba spin-orbit coupling are shown to exhibit a spin-selective Peierls-type transition into a mixed spin-charge-density-wave state. The transition leads to a gap for one-half of the conducting modes, which is strongly enhanced by electron-electron interactions. The other half of the modes remains in a strongly renormalized gapless state and conducts opposite spins in opposite directions, thus providing a perfect spin filter. The transition is driven by magnetic field and by spin-orbit interactions. As an example we show for semiconducting quantum wires and carbon nanotubes that the gap induced by weak magnetic fields or intrinsic spin-orbit interactions can get renormalized by 1 order of magnitude up to 10–30 K.

DOI: 10.1103/PhysRevB.82.045127 PACS number(s): 71.30.+h, 71.10.Pm, 71.70.Ej, 72.25.−b

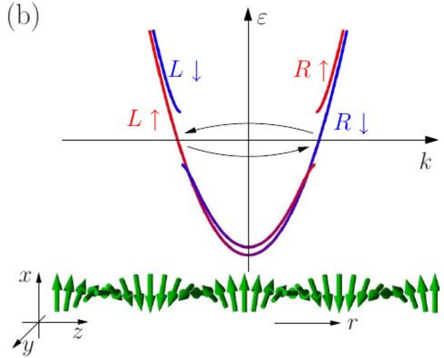

Spin spiral (helical) texture in experiments

PHYSICAL REVIEW B **85**, 020503(R) (2012)

Majorana fermions in superconducting nanowires without spin-orbit coupling

Morten Kjaergaard,[1] Konrad Wölms,[1,2] and Karsten Flensberg[1]
[1]*Niels Bohr Institute, University of Copenhagen, Universitetsparken 5, DK-2100 Copenhagen, Denmark*
[2]*Fachbereich Physik, Freie Universität Berlin, D-14195 Berlin, Germany*
(Received 11 November 2011; revised manuscript received 13 December 2011; published 13 January 2012)

We study nanowires with proximity-induced s-wave superconducting pairing in an external magnetic field that rotates along the wire. Such a system is equivalent to nanowires with Rashba-type spin-orbit coupling, with strength proportional to the derivative of the field angle. For realistic parameters, we demonstrate that a set of permanent magnets can bring a nearby nanowire into the topologically nontrivial phase with localized Majorana modes at its ends. This occurs even for a magnetic field configuration with nodes along the wire and alternating sign of the effective Rashba coupling.

DOI: 10.1103/PhysRevB.85.020503 PACS number(s): 74.78.Na, 73.63.Nm, 74.78.Fk

PHYSICAL REVIEW B **88**, 020407(R) (2013)

Proposal for realizing Majorana fermions in chains of magnetic atoms on a superconductor

S. Nadj-Perge, I. K. Drozdov, B. A. Bernevig, and Ali Yazdani*
Department of Physics, Joseph Henry Laboratories, Princeton University, Princeton, New Jersey 08544, USA
(Received 18 January 2013; published 25 July 2013)

We propose an easy-to-build easy-to-detect scheme for realizing Majorana fermions at the ends of a chain of magnetic atoms on the surface of a superconductor. Model calculations show that such chains can be easily tuned between trivial and topological ground states. In the latter, spatially resolved spectroscopy can be used to probe the Majorana fermion end states. Decoupled Majorana bound states can form even in short magnetic chains consisting of only tens of atoms. We propose scanning tunneling microscopy as the ideal technique to fabricate such systems and to probe their topological properties.

DOI: 10.1103/PhysRevB.88.020407 PACS number(s): 71.10.Pm, 03.67.Lx, 74.20.−z

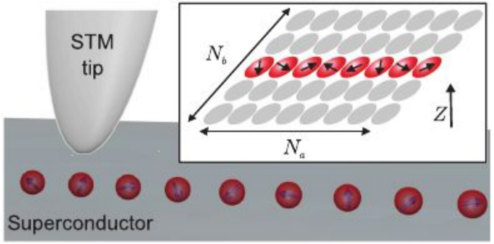

FIG. 1. (Color online) Schematic of the experimental setup. An array of magnetic atoms (red spheres) is assembled using a scanning tunneling microscope on the surface of the s-wave superconductor (gray background). The system is modeled by the two dimensional $N_a \times N_b$ array in which magnetic atoms are embedded (inset). Throughout the paper we consider the case where magnetic moments are in the plane defined by the N_a and Z directions.

Hamiltonian for spiral spin texture

$$\vec{S}_i = (S_i^x, S_i^y, S_i^z) = \frac{1}{2}\left(\cos\theta_i, \sin\theta_i, 0\right).$$

$$S_i^+ = \frac{z_i}{1+|z_i|^2}, \quad S_i^- = \frac{\bar{z}_i}{1+|z_i|^2}, \quad S_i^z = \frac{1}{2}\left(\frac{1-|z_i|^2}{1+|z_i|^2}\right).$$

$$H_{\text{eff}}(z,\xi) = -t\sum_i \xi_i\bar{\xi}_{i+1}a_{i,i+1} + \imath\alpha\sum_i \xi_i\bar{\xi}_{i+1}\alpha^*_{i,i+1} - \Delta\sum_i \xi_i\xi_{i+1}\Delta^*_{i,i+1} + \text{H.c.} + \mu\sum_i \bar{\xi}_i\xi_i, \quad (7)$$

where,

$$a_{i,i+1} \equiv \frac{1+\bar{z}_i z_{i+1}}{\sqrt{\left(1+|z_i|^2\right)\left(1+|z_{i+1}|^2\right)}}, \quad (8a)$$

$$\alpha^*_{i,i+1} \equiv \left[\frac{z_i-\bar{z}_{i+1}}{\sqrt{\left(1+|z_i|^2\right)\left(1+|z_{i+1}|^2\right)}}\right]^*, \quad (8b)$$

$$\Delta^*_{i,i+1} \equiv \left[\frac{z_i-z_{i+1}}{\sqrt{\left(1+|z_i|^2\right)\left(1+|z_{i+1}|^2\right)}}\right]^*. \quad (8c)$$

$$\begin{aligned} H_{\text{eff}} = &-t\sum_i \bar{\xi}_i\xi_{i+1}\cos\frac{(\theta_{i+1}-\theta_i)}{2} \\ &+\alpha\sum_i \bar{\xi}_i\xi_{i+1}\sin\frac{(\theta_{i+1}+\theta_i)}{2} \\ &-\Delta\sum_i \bar{\xi}_i\bar{\xi}_{i+1}\sin\frac{(\theta_{i+1}-\theta_i)}{2} + \text{H.c.} \\ &+\mu\sum_i \bar{\xi}_i\xi_i. \end{aligned}$$

Hamiltonian for spiral spin texture

$$
\begin{aligned}
H_{\text{eff}} = & -t\sum_i \bar{\xi}_i \xi_{i+1} \cos\frac{(\theta_{i+1}-\theta_i)}{2} \\
& + \alpha \sum_i \bar{\xi}_i \xi_{i+1} \sin\frac{(\theta_{i+1}+\theta_i)}{2} \\
& - \Delta \sum_i \bar{\xi}_i \bar{\xi}_{i+1} \sin\frac{(\theta_{i+1}-\theta_i)}{2} + \text{H.c.} \\
& + \mu \sum_i \bar{\xi}_i \xi_i .
\end{aligned}
$$

Constant angle between spin and without Rashba

For Constant change in angle between neighboring spin $\theta_{i+1} - \theta_i = \theta$

Without Rashba spin orbit coupling, the Hamiltonian will be:

$$H_{\text{eff}}^{\text{Kitaev}} = -t \sum_i \bar{\xi}_i \xi_{i+1} \cos\frac{\theta}{2} - \Delta \sum_i \bar{\xi}_i \bar{\xi}_{i+1} \sin\frac{\theta}{2} + \text{H.c.} + \mu \sum_i \bar{\xi}_i \xi_i .$$

The resulting Ham. is analogous to Kitaev Ham.

Our Hamiltonian

$$H_{\mathrm{eff}}^{\mathrm{Kitaev}} = -t \sum_i \bar{\xi}_i \xi_{i+1} \cos\frac{\theta}{2} - \Delta \sum_i \bar{\xi}_i \bar{\xi}_{i+1} \sin\frac{\theta}{2} + \mathrm{H.c.} + \mu \sum_i \bar{\xi}_i \xi_i .$$

Original Kitaev Hamiltonian

$$H = -\mu \sum_x c_x^\dagger c_x - \frac{1}{2} \sum_x \left(t c_x^\dagger c_{x+1} + \Delta e^{i\phi} c_x c_{x+1} + \mathrm{H.c.} \right),$$

The resulting Ham. is analogous to Kitaev Ham.

The only **difference** is the parametrized **hopping** $t\cos(\theta/2)$

and parametrized **superconducting gap** $\Delta\sin(\theta/2)$

Our Hamiltonian

$$H_{\text{eff}}^{\text{Kitaev}} = -t\sum_i \bar{\xi}_i \xi_{i+1} \cos\frac{\theta}{2} - \Delta \sum_i \bar{\xi}_i \bar{\xi}_{i+1} \sin\frac{\theta}{2} + \text{H.c.} + \mu \sum_i \bar{\xi}_i \xi_i .$$

Original Kitaev Hamiltonian

$$H = -\mu \sum_x c_x^\dagger c_x - \frac{1}{2} \sum_x (t c_x^\dagger c_{x+1} + \Delta e^{i\phi} c_x c_{x+1} + \text{H.c.}),$$

Condition for topological phase

Our Hamiltonian

Condition for topological phase

$$|\mu| < 2t\cos(\theta/2)$$

$$H_{\mathrm{eff}}^{\mathrm{Kitaev}} = -t\sum_i \bar{\xi}_i \xi_{i+1} \cos\frac{\theta}{2} - \Delta \sum_i \bar{\xi}_i \bar{\xi}_{i+1} \sin\frac{\theta}{2} + \mathrm{H.c.} + \mu \sum_i \bar{\xi}_i \xi_i .$$

Dependence of topological phase on angle

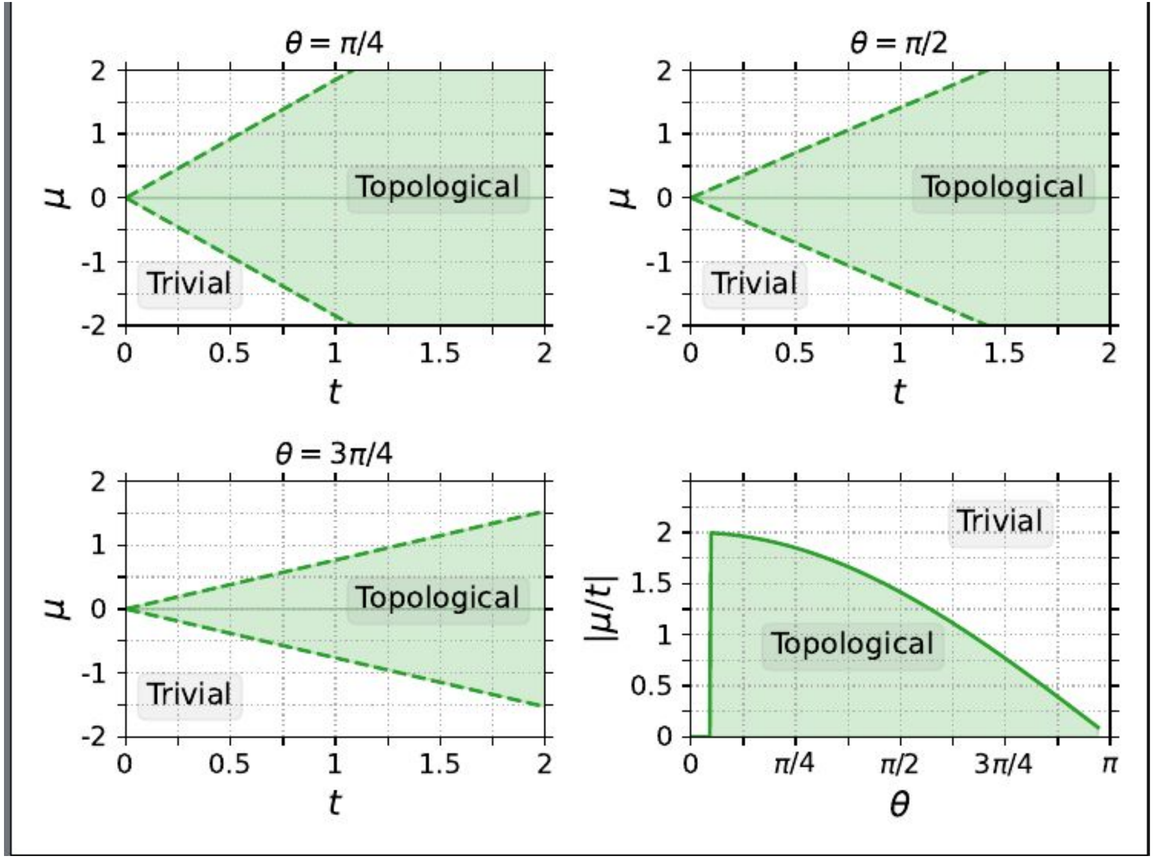

Energy dispersion relation

In the momentum space using Nambu operators the Hamitonian Eq. (14) can be written in usual Bogoliubov-de Gennes form:

$$H_{\mathrm{eff}}^{\mathrm{Kitaev}}(k) = \frac{1}{2}\sum_{k\in\mathrm{BZ}} \Psi_k^{\dagger}\,\mathcal{H}_k\,\Psi_k,$$

where,

$$\Psi_k^{\dagger} \equiv \left[\xi_k, \bar{\xi}_{-k}\right],$$

$$\mathcal{H}_k \equiv \begin{bmatrix} 2t\cos\frac{\theta}{2}\cos ka - \mu & 2\Delta\sin\frac{\theta}{2}\sin ka \\ 2\Delta\sin\frac{\theta}{2}\sin ka & 2t\cos\frac{\theta}{2}\cos ka - \mu \end{bmatrix} \tag{15}$$

The energy dispersion can easily be calculated:

$$E(k) = \pm\sqrt{\left(2t\cos\frac{\theta}{2}\cos ka - \mu\right)^2 + \left(2\Delta\sin\frac{\theta}{2}\sin ka\right)^2}. \tag{16}$$

Dependence of Free energy of system on chemical potential and angle, while superconducting gap is constant

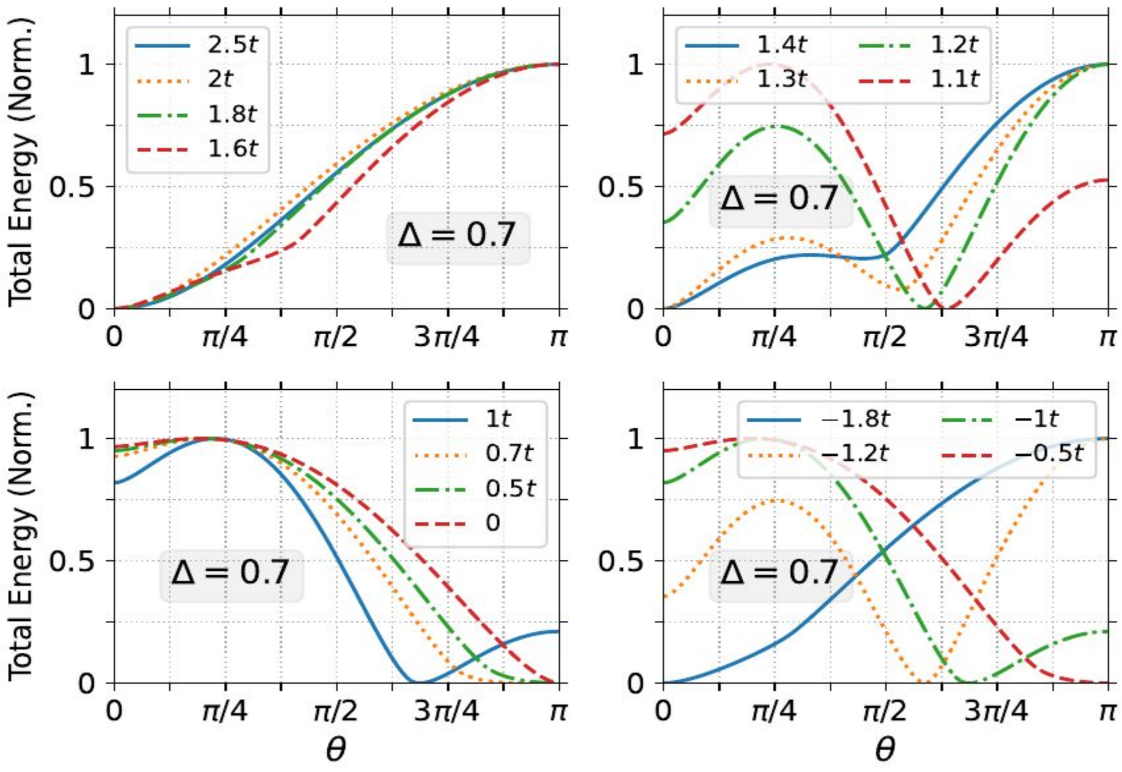

Dependence of Free energy of system on superconducting gap and angle, while chemical potential is constant

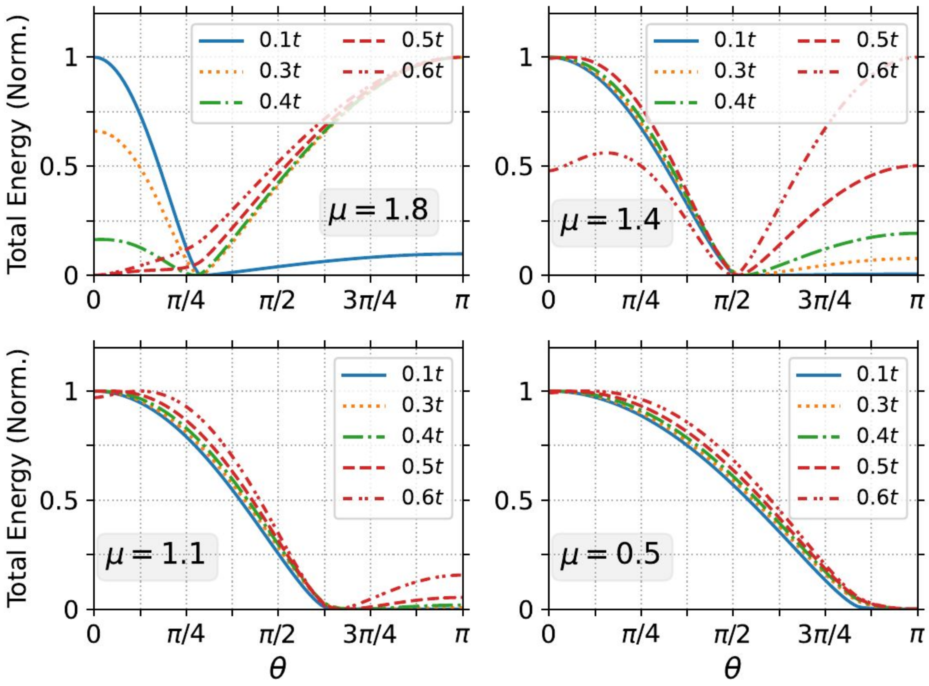

The Phase diagram of the parameters: chemical potential, superconducting gap and spin rotation angle

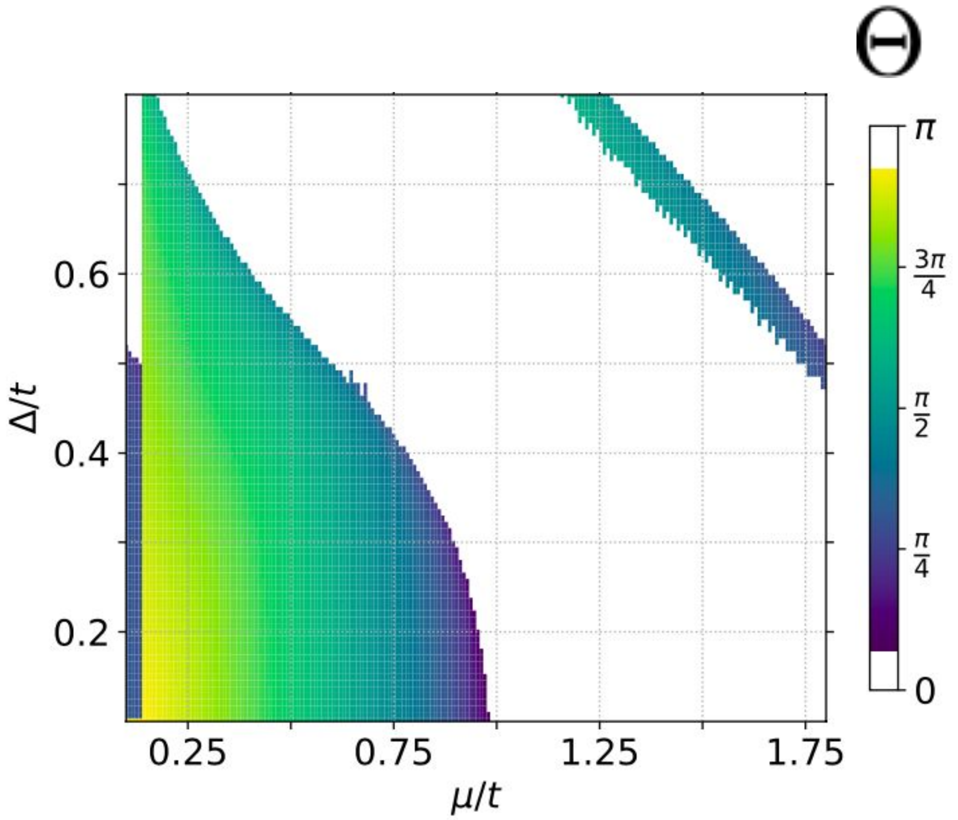

Hamiltonian with Rashba

$$H_{\text{eff}}(z,\xi) = -\sum_i \tilde{t}_i\, \bar{\xi}_i \xi_{i+1} - \Delta \sum_i \bar{\xi}_i \bar{\xi}_{i+1} \sin\frac{\theta}{2} + \text{H.c.} + \mu \sum_i \bar{\xi}_i \xi_i, \tag{17}$$

where

$$\tilde{t}_i \equiv \left[t\cos\left(\frac{\theta}{2}\right) - \alpha \sin\left(\theta_i + \frac{\theta}{2}\right)\right].$$

The hopping term has an **oscillating** character in the presence of Rashba

Topological properties with Rashba

$$|\mu| < \mathrm{Min.}(2\tilde{t}_i)$$

$$|\mu| < 2\left(t\cos\frac{\theta}{2} - |\alpha|\right). \qquad (18)$$

The effect of Rashba is to **decrease** the parameter space for **topological phase** in the phase of **chemical potential** and **hopping factors**.

Rashba decreases the parameter space for topological phase

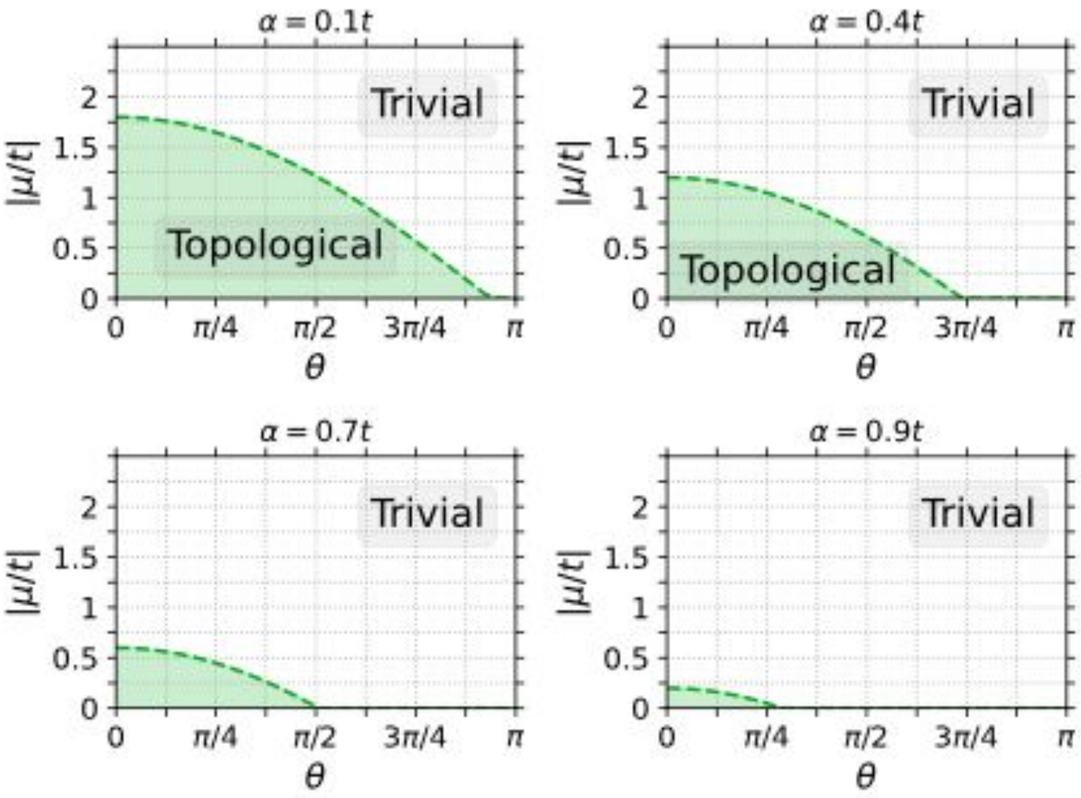

Proposed Experiments and Devices

Tunneling Experiments: thermodynamically induced spin texture

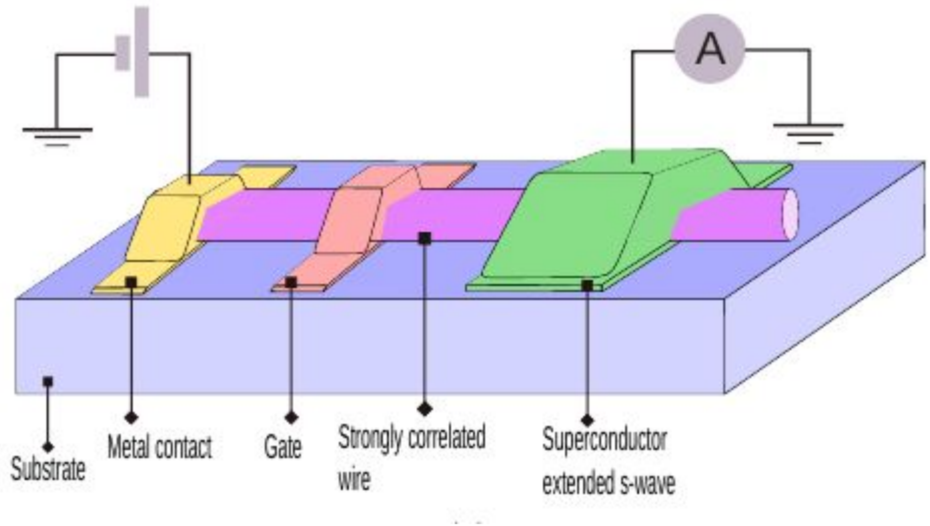

Tunneling Experiments: externally induced spin texture

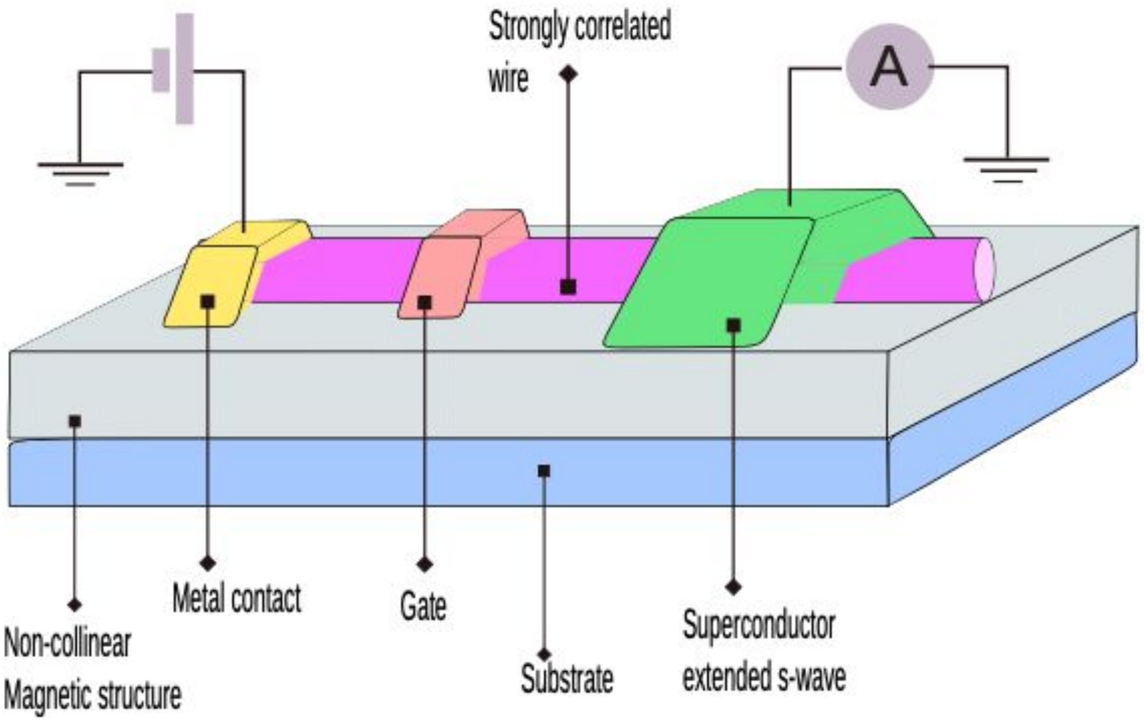

Tunneling Experiments:Materials

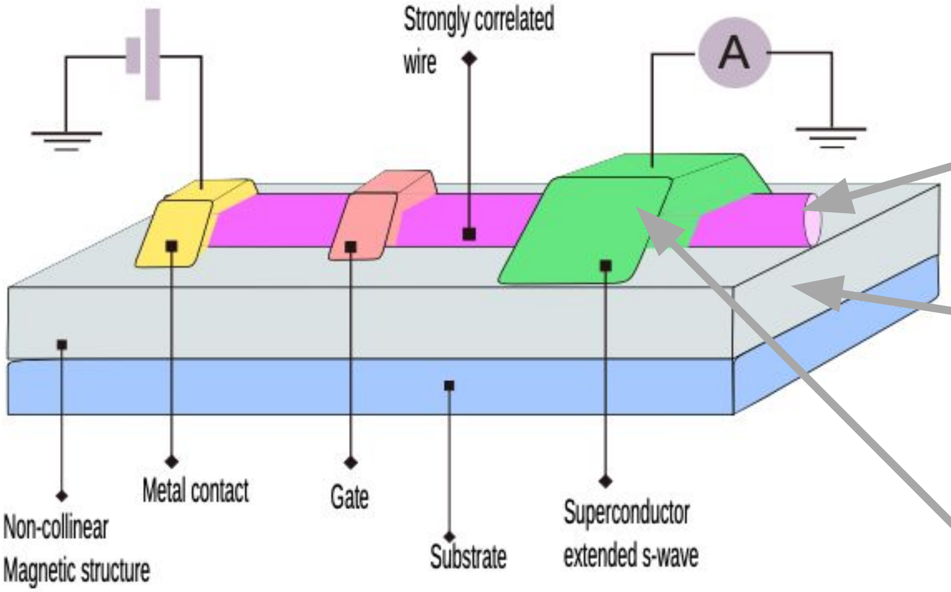

Heavy Fermion compounds
Transition Metal compounds
Transition metal dichalcognides

vdW and 2D magnetic materials

Iron based superconductors

Simple Device configuration

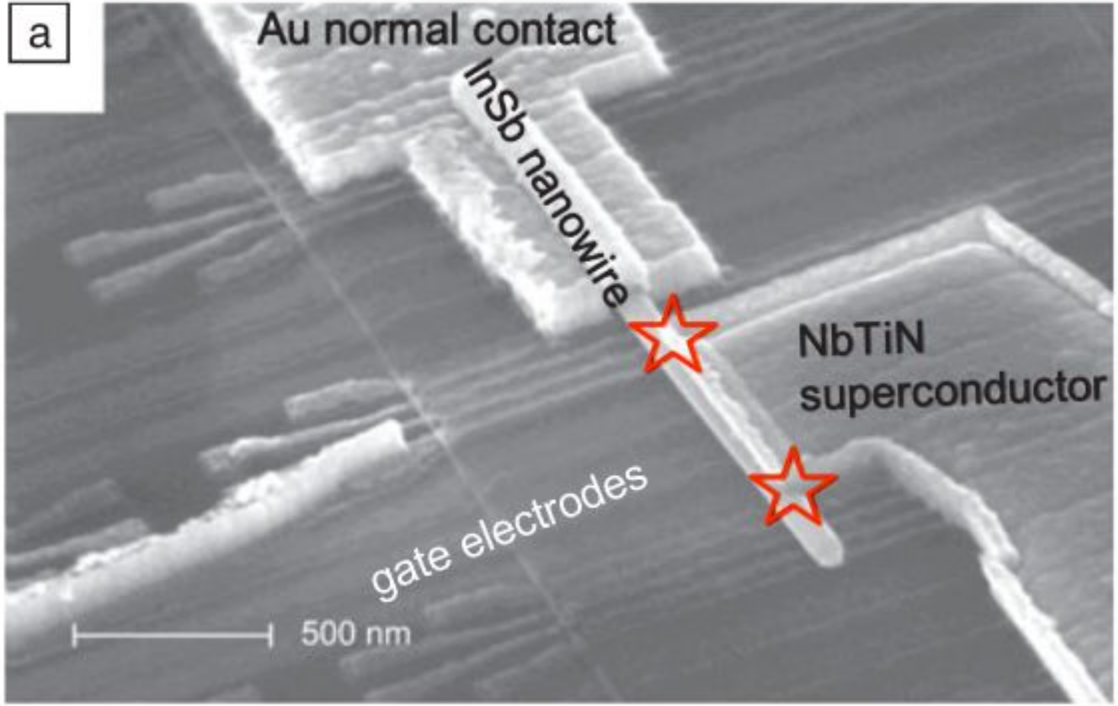

Conclusions

1. It was shown that **Majorana zero modes (MZM)** can appear in the strongly correlated wires without magnetic field.

2. Presences of the **Rashba** spin orbit **decreases** the **area** of the **parameter** space for **topological** phase. Hence, for **strongly correlated** wire Rashba spin orbit is **not necessary**. On the other hand in the usual semiconductor Majorona devices Rashba spin orbit was the **necessary** ingredient.

3. We show that for **suitable** values of **chemical potential** (\mu) and **superconducting gap** (\Delta) the system has **lowest** energy for angles **not** equal to zeros **(Ferromagnetic)** of pi **(Anti ferromagnetic)**.

4. We have proposed a **tunneling experiment** and **device design** for initial experiments involving strongly correlated nano wires.

Appendix

The Hamiltonian of the wire

Due to **proximity effect** superconductivity will also be induced in the nano wire.

Both **Andreev reflection** and **coherent propagation** of the superconducting pairs are responsible for induced superconductivity.

We assume **superconducting coherence length** is of **same order** as the **radius of the wire** ($\xi_{\text{wire}} \sim r$).

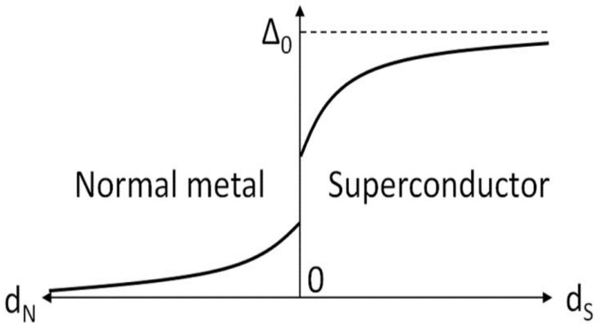

Coherent propagation

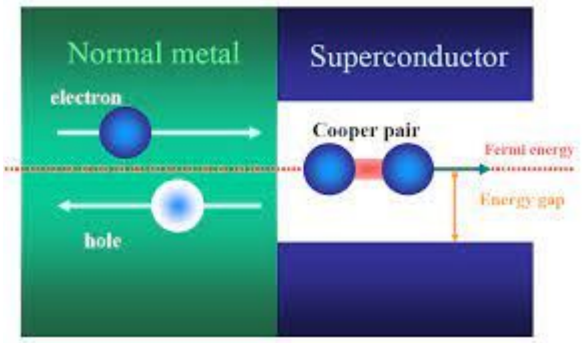

Andreev Reflection

Fermions, Bosons and **Anyons in 2D**!

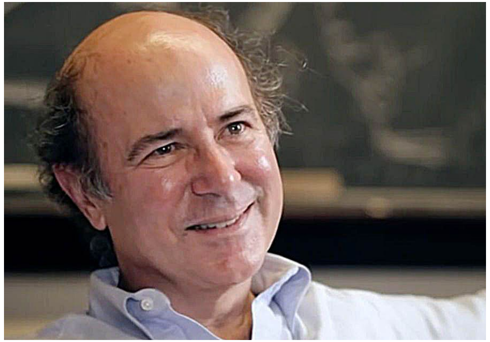

Frank Wilczek

In **2D** exchange of two particles will give the wave function an **arbitrary phase** factor. However, in **3D** this phase factor can only be **0 or \Pi.**

VOLUME 48, NUMBER 17 PHYSICAL REVIEW LETTERS 26 APRIL 1982

Magnetic Flux, Angular Momentum, and Statistics

Frank Wilczek
Institute for Theoretical Physics, University of California, Santa Barbara, California 93106
(Received 8 January 1982)

It is demonstrated that the orbital angular momentum l_z of a particle of charge q orbiting around a tube with magnetic flux Φ is quantized in units $l_z = \text{integer} - q\Phi/2\pi$. A very simple physical argument for this is presented, and applied to understand the Dirac quantization condition and the charge-spin relation for particles bound to magnetic monopoles. The unusual statistics of flux-tube–charged-particle composites is discussed.

PACS numbers: 14.80.Hv, 03.65.Bz

VOLUME 53, NUMBER 7 PHYSICAL REVIEW LETTERS 13 AUGUST 1984

Fractional Statistics and the Quantum Hall Effect

Daniel Arovas
Department of Physics, University of California, Santa Barbara, California 93106

and

J. R. Schrieffer and Frank Wilczek
Department of Physics and Institute for Theoretical Physics, University of California, Santa Barbara, California 93106
(Received 18 May 1984)

The statistics of quasiparticles entering the quantum Hall effect are deduced from the adiabatic theorem. These excitations are found to obey fractional statistics, a result closely related to their fractional charge.

What Makes an Anyon?

Imagine a particle looping around another. In three dimensions, that loop can shrink to a point, which is topologically equivalent to there being no loop at all. Accordingly, the particle's mathematical description (or wave function) is highly constrained. In two dimensions, however, the loop cannot shrink to a point, so the particle is not as constrained. Since "anything goes," these 2D particles are called anyons.

3D

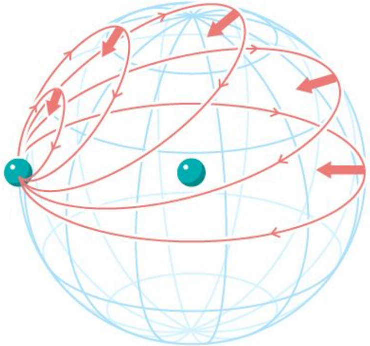

In 3D, a loop can shrink to a point.

2D

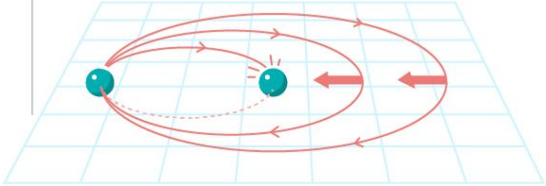

In 2D, the loop gets caught on the other particle.

The first mention of Majorona Fermions

1937

Ettore Majorona

Majorona intended this idea for application in particle physics, especially, he proposed **neutrinos to be its own antiparticle.** However, until now experimentally it is **not found**. Supersymmetric theories proposes that, bosonic particles like **photons** might be **Majorona particles**.

However !!!

In condensed matter physics **interaction induced excitations** can be thought as **particle**, hence, ingenious combination of **symmetries and excitations** can give rise to Majorona particles.

The first mention of Majorona Fermions

1937

Majorana, E. (1937) Il Nuovo Cimento, 5, 171-184.

Ettore Majorona

Predicted that some particles may constitute their own particles.

Mathematically:
If ***a*** is some operator of **Majorona particle** then:

$$a = a^{\dagger}$$

Majorona intended this idea for application in particle physics, especially, he proposed **neutrinos to be its own antiparticle.** However, until now experimentally it is **not found**. Supersymmetric theories proposes that, bosonic particles like **photons** might be **Majorona particles**.

The main results

<u>The System</u>

We consider a 1D nanowire with **strong correlation** on the ***extended s***-wave superconductor.

<u>The Results</u>

1. Majorona Fermions can appear **without**:
   a. **Magnetic field**
   b. **Rashba spin orbit interactions**
2. Gives another parameter, **the change in spin projection**, to control the

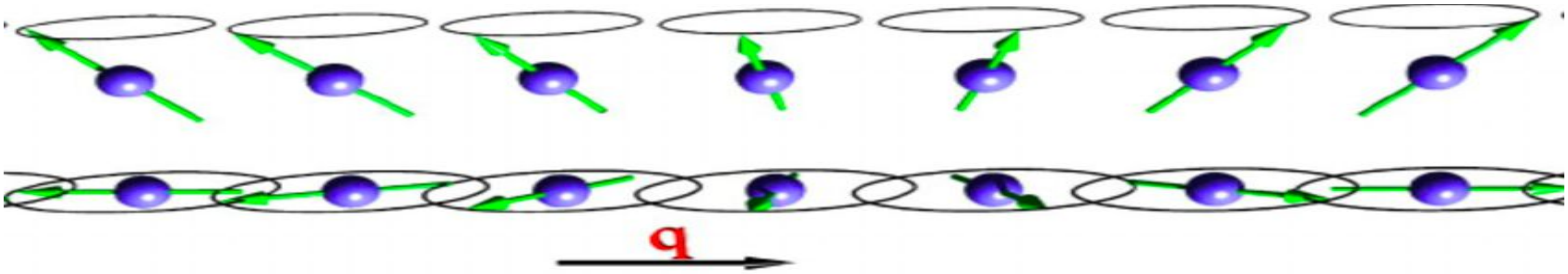

The main results

The System

We consider a 1D nanowire with **strong correlation** on the ***extended s***-wave superconductor.

The Results

1. Majorona Fermions can appear **without**:
   a. **Magnetic field**
   b. **Rashba spin orbit interactions**
2. Gives another parameter, **the change in spin projection**, to control the topological phase in the system.
3. Proposal of synthesizing new devices, **with less demanding material parameters.**

Majorona zero-modes (MZM) in 2D systems

1999

G. E. Volovik

G. E. Volovik,JETP Letters,70,609–614

2008

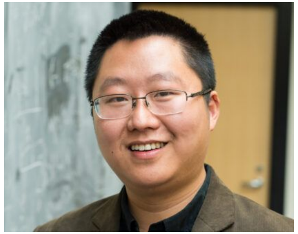

Liang Fu

Charles Kane

Liang Fu and C. L. Kane, Phys. Rev. Lett. 100, 096407

2010

Jay D. Sau

Sankar Das Sarma

Jay D. Sau et. al., Phys. Rev. Lett. 104, 040502

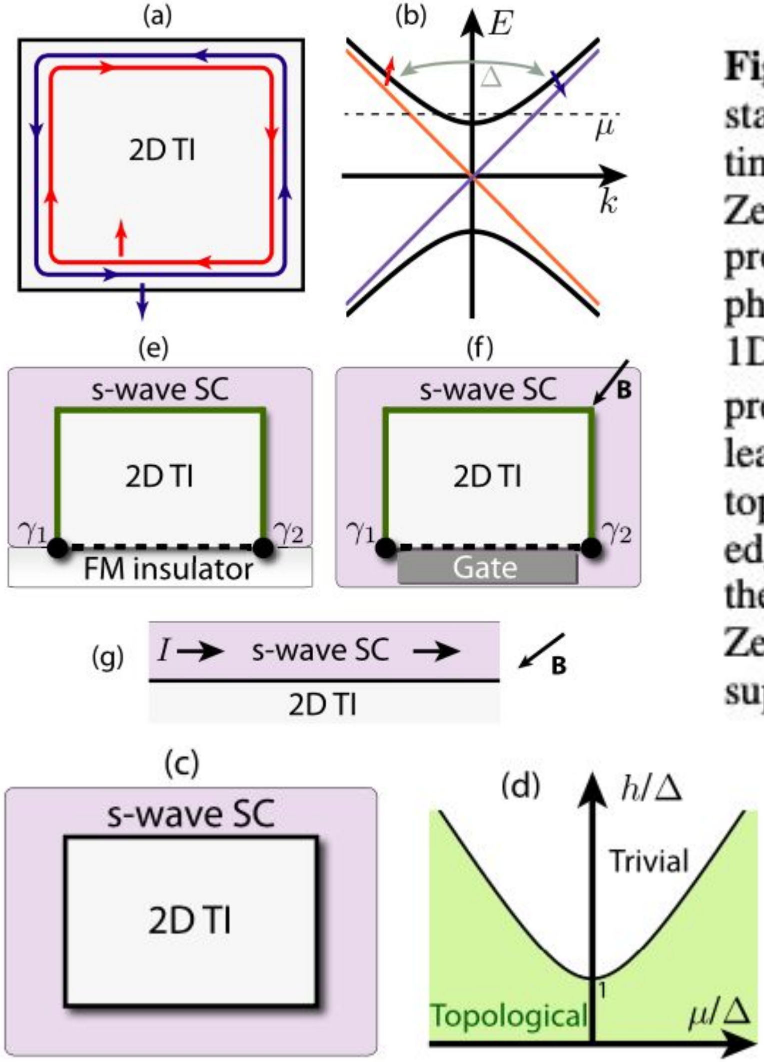

Figure 5. (*a*) Schematic of counter-propagating, spin-filtered edge states in a 2D topological insulator. (*b*) Edge-state dispersion when time-reversal symmetry is present (red and blue lines) and with a Zeeman field h of the form in equation (55) (solid curves). (*c*) A proximate s-wave superconductor drives the edge into a topological phase similar to the weak-pairing phase in Kitaev's toy model for a 1D spinless p-wave superconductor. When the Zeeman field h is present, the topological phase survives provided $h < \sqrt{\Delta^2 + \mu^2}$ leading to the phase diagram in (d). Domain walls between topological (green lines) and trivial regions (dashed lines) on the edge trap localized Majorana zero-modes. As described in the text these can be created with (*e*) a ferromagnetic insulator, (*f*) a Zeeman field combined with electrostatic gating or (*g*) applying supercurrents near the edge.

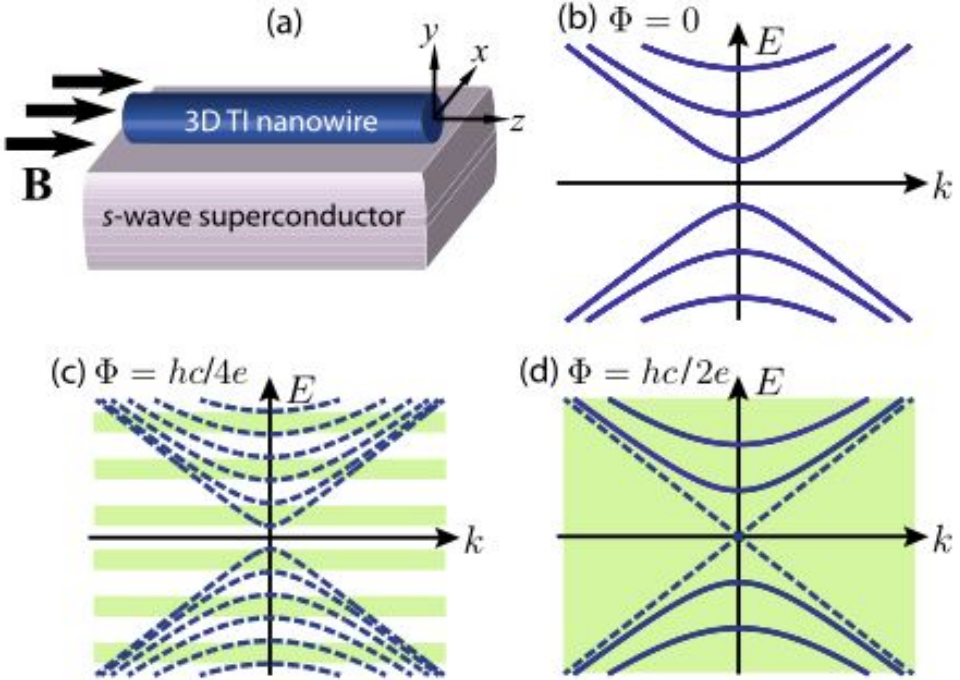

Figure 7. (*a*) A 3D topological insulator nanowire with a magnetic field applied along its axis can realize a topological superconducting state when in contact with an s-wave superconductor. (*b*)–(*d*) Nanowire band structure when the flux Φ passing through its center is (*b*) 0, (*c*) $hc/4e$, and (*d*) $hc/2e$. Solid and dashed curves respectively denote doubly degenerate and non-degenerate bands. Green shaded regions indicate chemical potential windows in which an odd number of channels is occupied, as required for generating topological superconductivity.

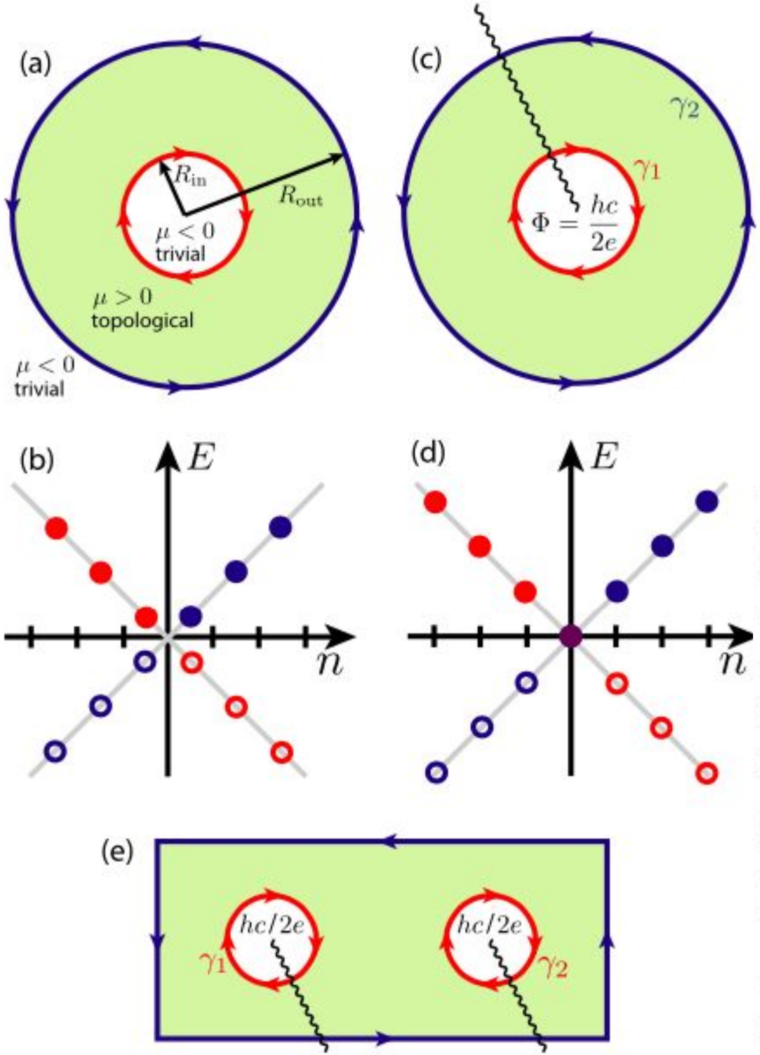

Figure 4. (*a*) A topological $p + \mathrm{i}p$ superconductor on an annulus supports chiral Majorana edge modes at its inner and outer boundaries. (*b*) Energy spectrum versus angular momentum n for the inner (red circles) and outer (blue circles) edge states in the setup from (*a*). Here n takes on half-integer values because the Majorana modes exhibit anti-periodic boundary conditions on the annulus. An $hc/2e$ flux piercing the central trivial region as in (*c*) introduces a branch cut (wavy line) which, when crossed, leads to a sign change for the Majorana edge modes. The flux therefore changes the boundary conditions to periodic and shifts n to integer values. This leads to the spectrum in (*d*), which includes Majorana zero-modes γ_1 and γ_2 localized at the inner and outer edges. The two-vortex setup in (*e*) supports one Majorana zero-mode localized around each puncture, while the outer boundary remains gapped.

Origin of spin–orbit coupling. When an electron with momentum $\mathbf{p}$ moves in a magnetic field $\mathbf{B}$, it experiences a Lorentz force in the direction perpendicular to its motion $\mathbf{F} = -e\mathbf{p} \times \mathbf{B}/m$ and possesses Zeeman energy $\mu_B \boldsymbol{\sigma} \cdot \mathbf{B}$, where $\boldsymbol{\sigma}$ is the vector of the Pauli spin matrices, m and e are the mass and charge of the electron, respectively, and $\mu_B = 9.27 \times 10^{-24}$ J T^{-1} is the Bohr magneton. By analogy, when this electron moves in an electric field $\mathbf{E}$, it experiences a magnetic field $\mathbf{B}_{\mathrm{eff}} \sim \mathbf{E} \times \mathbf{p}/mc^2$ in its rest-frame (where c is the speed of light) — a field that also induces a momentum-dependent Zeeman energy called the SO coupling, $\hat{H}_{\mathrm{SO}} \sim \mu_B (\mathbf{E} \times \mathbf{p}) \cdot \boldsymbol{\sigma}/mc^2$. In crystals, the electric field is given by the gradient of the crystal potential $\mathbf{E} = -\nabla V$, which produces a SO field $\mathbf{w}(\mathbf{p}) = -\mu_B(\nabla V \times \mathbf{p})/mc^2$. Because SO coupling preserves time-reversal symmetry ($\mathbf{w}(\mathbf{p}) \cdot \boldsymbol{\sigma} = -\mathbf{w}(-\mathbf{p}) \cdot \boldsymbol{\sigma}$), the SO field must be odd in electron momentum $\mathbf{p}$; that is, $\mathbf{w}(-\mathbf{p}) = -\mathbf{w}(\mathbf{p})$. This odd-in-$p$ SO field only survives in systems that lack spatial inversion symmetry.

Dresselhaus and Rashba spin–orbit coupling. Dresselhaus[1] was the first to notice that in zinc-blende III–V semiconductor compounds lacking a centre of inversion, such as GaAs or InSb, the SO coupling close to the Γ point adopts the form

$$\hat{H}_{D_3} = (\gamma/\hbar)\,((p_y^2 - p_z^2)p_x\sigma_x + \text{c.p.}) \quad (1)$$

where c.p. denotes circular permutations of indices. Of course, additional symmetry considerations in the band structure result in additional odd-in-p SO coupling terms (see for example, ref. 136). In the presence of strain along the (001) direction, the cubic Dresselhaus SO coupling given in equation 1 reduces to the linear Dresselhaus SO coupling[137]

$$\hat{H}_{D_1} = (\beta/\hbar)\,(p_x\sigma_x - p_y\sigma_y) \quad (2)$$

where $\beta = \gamma p_z^2$. In quantum wells with structural inversion symmetry broken along the growth direction and respecting the C_{2v} symmetry, Vas'ko[3] and Bychkov and Rashba[4] proposed that the interfacial electric field $\mathbf{E} = E_z\mathbf{z}$ results in a SO coupling of the form

$$\hat{H}_R = (\alpha_R/\hbar)\,(\mathbf{z} \times \mathbf{p}) \cdot \boldsymbol{\sigma} \quad (3)$$

where α_R is known as the Rashba parameter. In other words, in the solid state the Dirac gap $mc^2 \approx 0.5$ MeV is replaced by the energy gap ~1 eV between electrons and holes, and $\alpha_R/\hbar \gg \mu_B E_z/mc$. This convenient form, derived for 2D plane waves, is only phenomenological and must be applied with precaution to realistic systems. Indeed, theoretical investigations showed that the lack of inversion symmetry does not only create an additional electric field E_z, but also distorts the electron wavefunction close to the nuclei, where the plane-wave approximation is not valid[138]. Therefore, for the discussion provided in this Review, one must keep in mind that the p-linear Rashba SO coupling is a useful approximation that does not entirely reflect the actual form of the SO coupling in inversion-asymmetric systems.

Both Dresselhaus and Rashba SO coupling lock spin to the linear momentum and split the spin sub-bands in energy (Fig. 2a). Such band splitting is also observed at certain metallic surfaces (Fig. 2b). The illustration below shows the spin texture at the Fermi surface in the case of Rashba (panel **a**) and strain-induced (panel **b**) p-linear Dresselhaus SO coupling. In the example shown in panel **c**, when both are present with equal magnitude, the SO field aligns along the [110] direction, resulting in, for instance, the suppression of spin relaxation interaction in this direction[43].

2D Majorana devices **based on topological insulators (TI)**

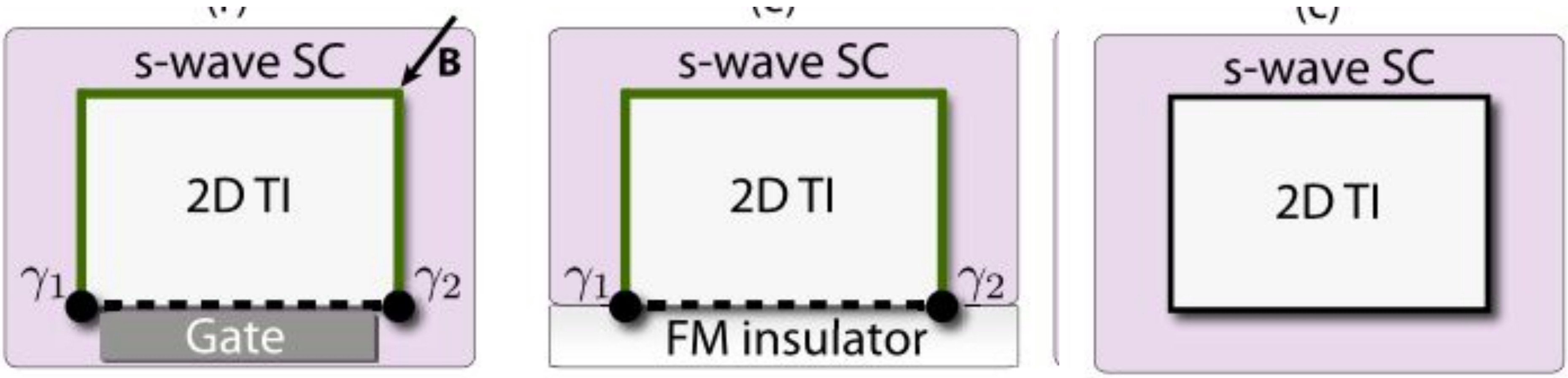

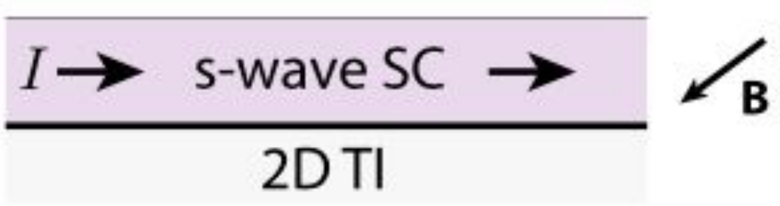

Fu L and Kane C L 2008 Phys. **Rev. Lett. 100 096407**
Fu L and Kane C L 2009 **Phys. Rev. B 79 161408(R)**

2D Majorana devices **based on ferromagnetic materials (FM)**

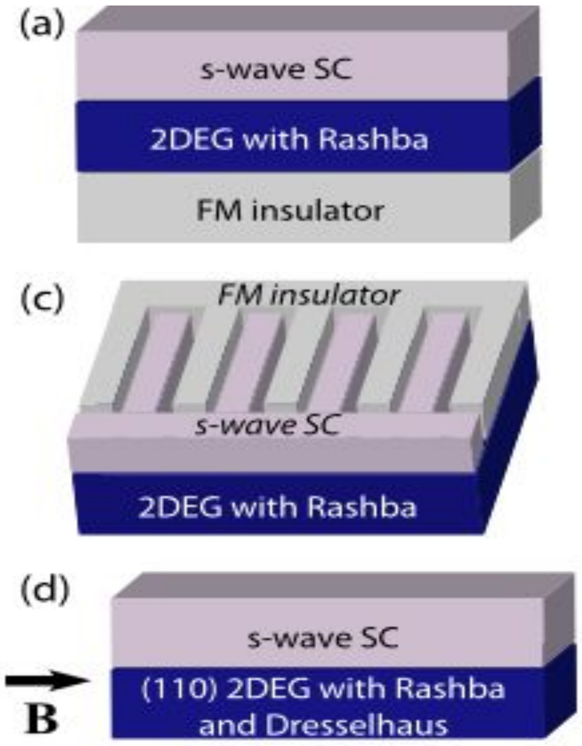

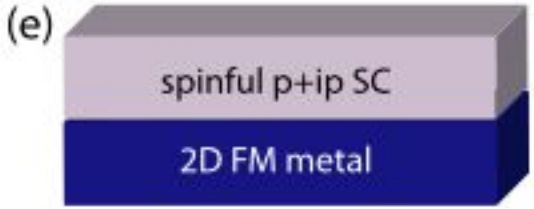

Alicea J 2010 **Phys.Rev.B 81125318**

Lee S-P, Alicea J and Refael G 2012, **arXiv:1205.3185**

Chung S B, Zhang H-J, Qi X-L and Zhang S-C 2011 **Phys. Rev. B 84 060510**

Lee P A 2009, **arXiv:0907.2681**

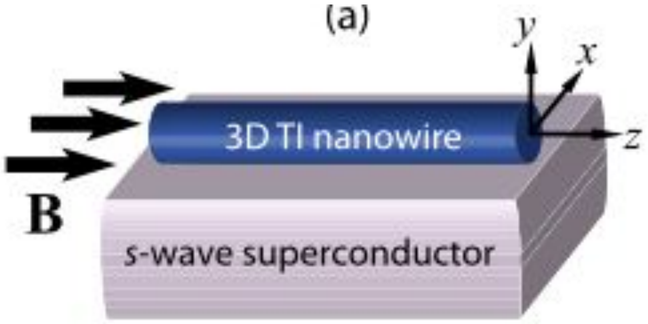

Cook A and Franz M 2011 Phys. Rev. B 84 201105

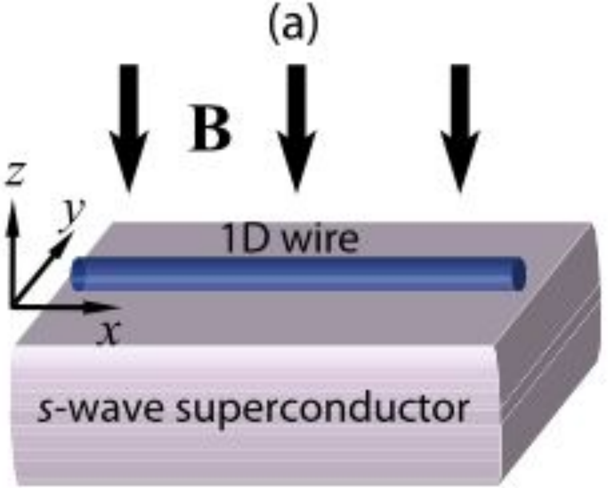

Lutchyn R M, Sau J D and Das Sarma S 2010 Phys.Rev.Lett. 105 077001

Oreg Y, Refael Gandvon Oppen F 2010 Phys.Rev.Lett. 105 177002

Rashba field and spin precession. When the electron spin is not aligned with the Rashba field, spin precession takes place with a frequency that depends on the magnitude of the field. In the bottom panel, the spin-polarized electrons injected along the x axis precess under the influence of the Rashba field, even without an applied magnetic field. The magnitude of the electric field, and hence the strength of the Rashba field and spin precession rate, can be controlled by a gate voltage[23,31–33] (Fig. 2c). In the diffusive regime, this precession is at the origin of the Dyakonov–Perel spin-relaxation mechanism[42]. An interesting consequence of the emergence of the Rashba field is the possibility to polarize flowing electrons along the direction of this field. This is known as the inverse spin galvanic effect[28]. This effect has a counterpart referred to as the spin galvanic effect[25], in which non-equilibrium spin density (created by either optical or electrical means) is converted into a charge current.

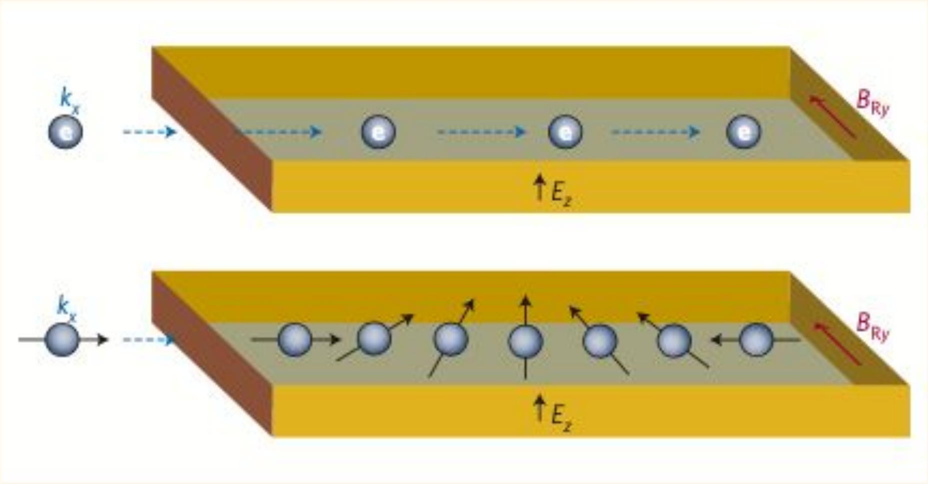

Inverse spin galvanic effect and spin precession. Top: Moving electrons (k_x) with a perpendicular electric field (E_z) experience the Rashba field, B_{Ry}. Bottom: In a Rashba system, the spin of the moving electrons (arrows) precesses around the axis of the Rashba field.

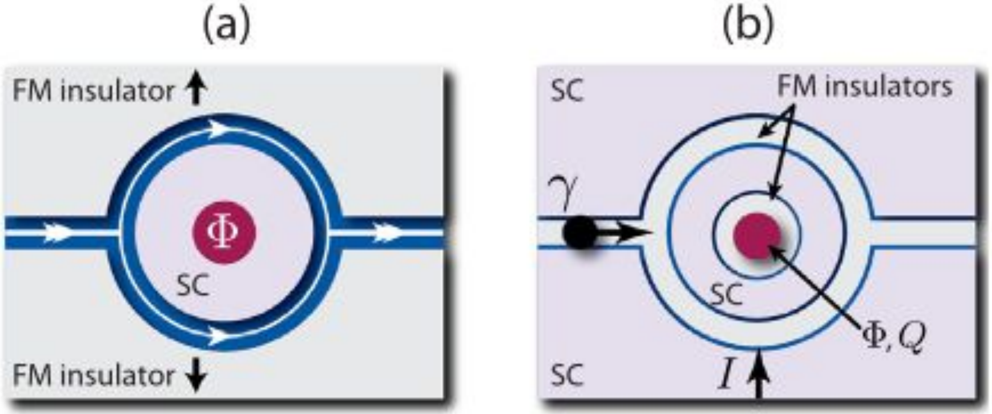

Figure 12. Interferometers fabricated from ferromagnetic insulators and s-wave superconductors deposited on a 3D topological insulator surface. In (*a*) the ferromagnets have opposite magnetizations, yielding a conventional chiral edge state (double arrows) that fractionalizes into chiral Majorana modes (single arrows) around the superconductor. With a flux $\Phi = (hc/2e)N_v$ threading the center, the zero-bias conductance describing current flow from the left domain wall into the superconductor vanishes for even N_v and is quantized at $2e^2/h$ for odd N_v. In (*b*), when $\Phi = 0$ Josephson vortices flowing through the interferometer produce a vortex current that oscillates with the charge Q on the central island (due to the Aharonov–Casher effect). When $\Phi = hc/2e$, however, the oscillations disappear as a consequence of non-Abelian statistics.

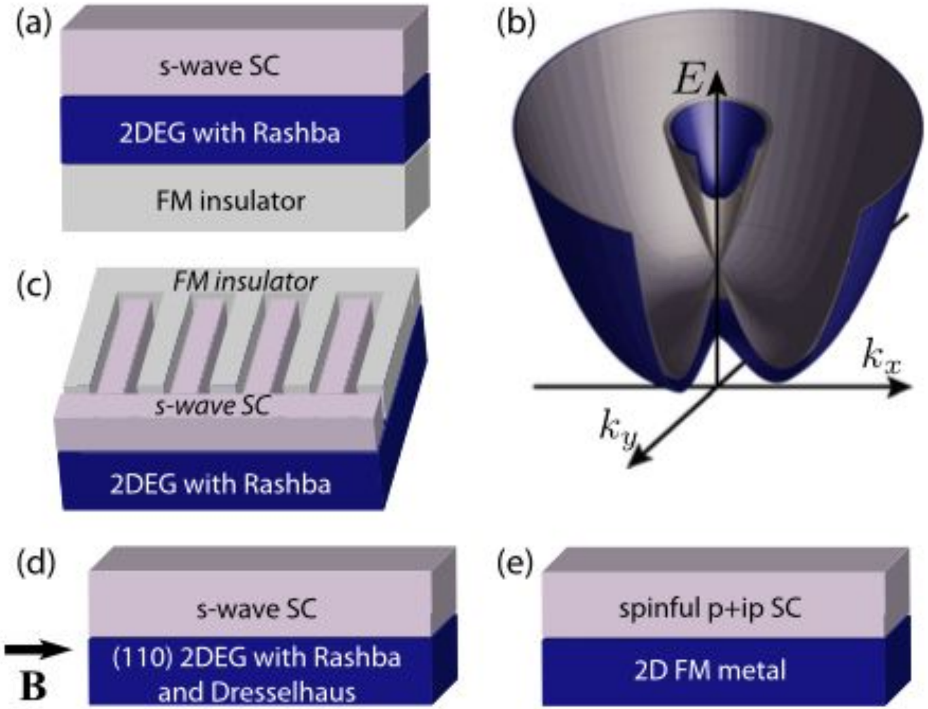

Figure 9. (*a*) A 2DEG with Rashba spin–orbit coupling can effectively realize a topological 2D 'spinless' $p + \mathrm{i}p$ superconductor when in contact with a ferromagnetic insulator and conventional s-wave superconductor. (*b*) Band structure for the 2DEG when time-reversal symmetry is present (gray) and with a non-zero Zeeman field (blue) that opens up a 'spinless' regime. (The break in the spectrum appears for clarity.) Alternative devices that support topological phases appear in (*c*)–(*e*).

The main result

In our proposed system the Majorana Fermions can appear **without**:

a. **Magnetic field**
b. **Rashba spin orbit interactions**

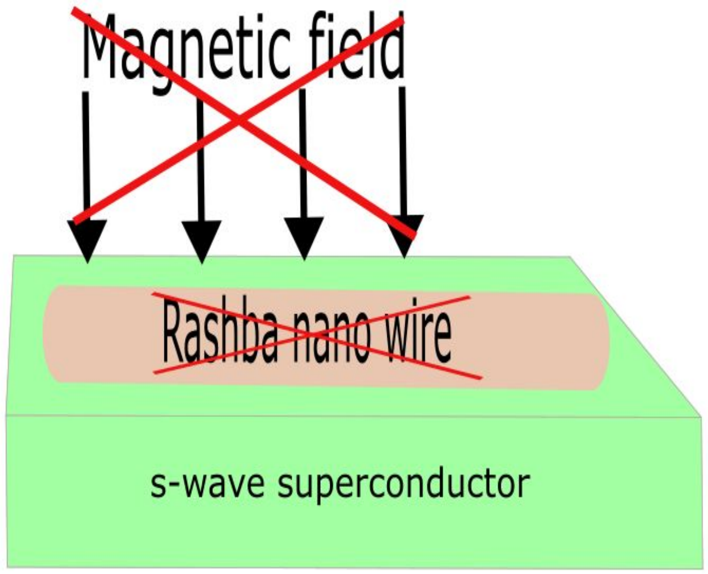

Processes of proximity induced superconductivity

Both **Andreev reflection** and **coherent propagation** of the superconducting pairs are responsible for induced superconductivity.

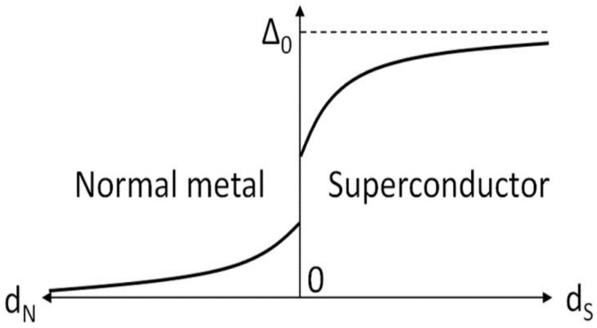

Coherent propagation

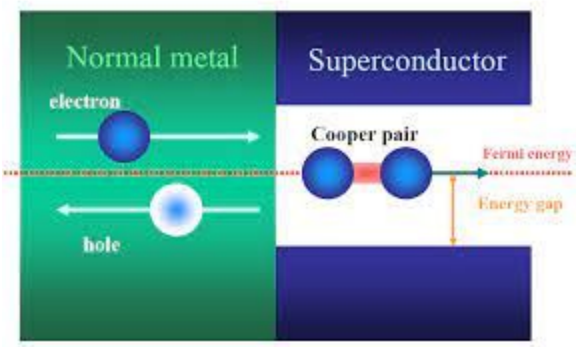

Andreev Reflection

Proximity induced superconducting in wire

Due to **proximity effect** superconductivity will also be induced in the nano wire.

We assume **superconducting coherence length** is of **same order** as the **radius of the wire** ($\xi_{\rm wire} \sim r$).

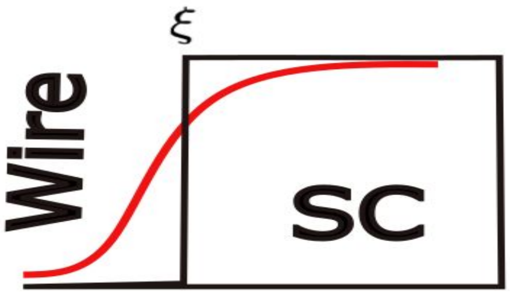

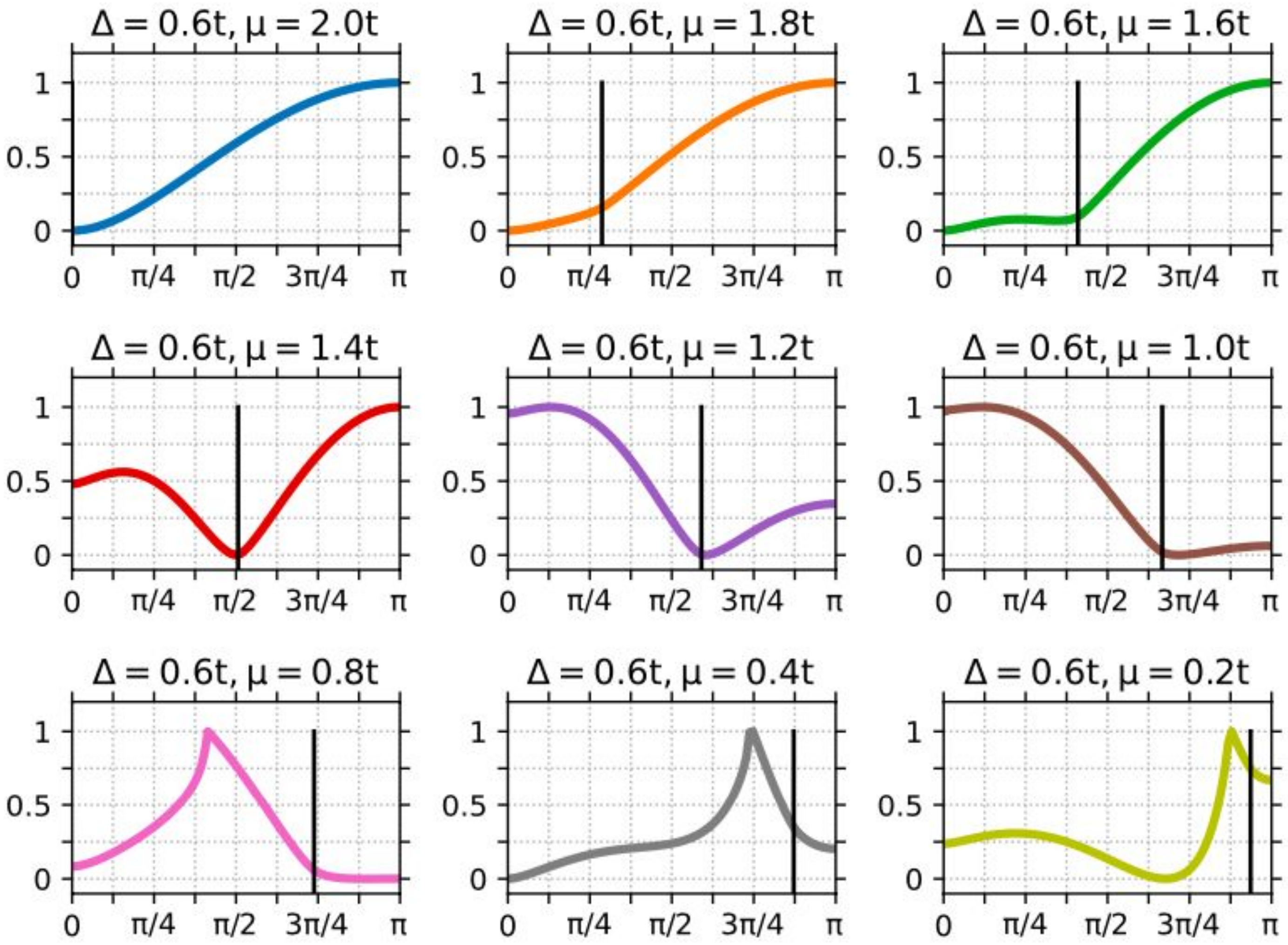
Δ = 0.6t, μ = 2.0t
Δ = 0.6t, μ = 1.8t
Δ = 0.6t, μ = 1.6t
Δ = 0.6t, μ = 1.4t
Δ = 0.6t, μ = 1.2t
Δ = 0.6t, μ = 1.0t
Δ = 0.6t, μ = 0.8t
Δ = 0.6t, μ = 0.4t
Δ = 0.6t, μ = 0.2t
0
0.5
1
0
π/4
π/2
3π/4
π